Molecular Crystals and Liquid Crystals
Publication details, including instructions for authors and subscription information:
http://www.tandfonline.com/loi/gmcl16

Exciton Percolation, Tunneling and Thermalization

E. M. Monberg [a a] & R. Kopelman [a]
[a] Department of Chemistry, The University of Michigan, Ann Arbor, Michigan, 48109, U.S.A.
Version of record first published: 14 Oct 2011.

To cite this article: E. M. Monberg & R. Kopelman (1980): Exciton Percolation, Tunneling and Thermalization, Molecular Crystals and Liquid Crystals, 57:1, 271-312

To link to this article: http://dx.doi.org/10.1080/00268948008069831

Mol. Cryst. Liq. Cryst., 1980, Vol. 57, pp. 271–312
0026-8941/80/5701–0271$04.50/0

Printed in U.S.A.

Exciton Percolation, Tunneling and Thermalization

Naphthalene first singlet and triplet†

E. M. MONBERG‡ and R. KOPELMAN

Department of Chemistry, The University of Michigan, Ann Arbor, Michigan 48109, U.S.A.

New experimental data are presented for triplet and singlet naphthalene exciton transport in ternary molecular crystals: isotopic mixed guest–host systems with a small added amount of sensor (supertrap). The focus is on the effects of the following parameters: Time, temperature, concentration and energy denominators (for guest–host, guest–guest, and guest–sensor energy levels). We find that, under the proper conditions, both singlet and triplet measurements are consistent with a *dynamic* exciton percolation model, i.e. where a guest cluster is defined by the extent of *long-range* exciton-superexchange (tunneling) interactions, and where the interaction cut-off is determined by the overall time available for transport (i.e., the lifetime of the excitation). The roles of temperature, lattice heterogeneity, and suggested models involving an Anderson–Mott mobility edge are discussed. We also emphasize the distinction between intra and inter-domain energy transfer and discuss the localization vs. delocalization dichotomy as well as dynamic vs. static percolation.

INTRODUCTION

Broude's main studies involved Frenkel exciton states. First he and his collaborators studied neat crystals, then dilute isotopic mixed crystals, then concentrated isotopic mixed crystals, eventually emphasizing the concept of cluster states.[1] Understanding these static states is a prerequisite for the study of exciton dynamics. The concepts of clusters and cluster percolation, and the related dichotomy between localized and extended states were first applied to excitons in such static studies primarily involving theoretical formulations, computer simulations and absorption experiments.[2] Going one step further we would expect the concepts of clusters and cluster percolation to

† Supported by NIH Grant No. 2 R01 NS08116-10A1.
‡ Western Electric, Engineering Research Center, P.O. Box 900, Princeton, N.J. 08540.

play an important role in energy transport. While attempts have been made recently[3,4] to interpret critical energy transport experiments,[5–7] in terms of mean field or effective medium type theories (i.e. ignoring clusterization), we believe that neither the (static) Anderson–Mott mobility edge approach,[3,8–11] nor the (dynamic) diffusion approach[3c,4] can be satisfactory, without explicitly incorporating the concepts of clusters and percolation. We give below our suggested models for both "static" and "dynamic" critical energy transport (i.e. energy transport characterized by a critical concentration, critical exponents, etc.) in conjunction with related experimental studies. Specifically, we point out in which domains an "analog Anderson transition" (quasistatic percolation) or an "analog diffusion" (dynamic percolation) model account for the experimental observations in our binary naphthalene system. We notice that for the situation where the energy transport is essentially restricted to one component in a substitutionally random binary lattice, neither the traditional Anderson model,[12] nor the traditional diffusion model[13] are expected to be pertinent.[14] Experimentally, we utilize the parameter of temperature to show the transition from a quasistatic to a dynamic percolation regime, emphasizing the important role of the various activation energies and their relation with the cluster structure and percolation. Other experimental parameters include the excitation lifetime, activation energies, energy denominators and the concentrations of both guest and sensor.

PRELIMINARY DISCUSSION

Static and dynamic clusters

The study of any conductor-insulator type transition is fraught with both conceptual and practical pitfalls. The case of Frenkel excitons is a good example. The question is: How and when does one encounter "localized" states?

One can assume a "micro-classical" model where the exciton transport occurs only between *nearest-neighbor* lattice sites. If we now randomly substitute exciton "conducting" sites with vacancies or exciton-insulating (non-conducting) sites, then the question of transport becomes primarily a problem of connectivity. If the concentration of conducting sites falls below the *critical concentration* defined by *percolation theory*,[15] we have an insulator. The value of this critical concentration depends on the topology of the lattice (i.e., the "coordination number" and dimensionality of the nearest neighbor bonds). This model can be refined by specifying

1) the domain size confining the transport,

2) the relaxation of the requirement of interaction with nearest neighbor only bonds (resulting in long-range percolation[16])

3) a restriction on the total number of site-to-site "hops".

One can also work with a ("quantum mechanical") model based on a transition from a "conducting" energy band to a "non-conducting" set of discrete eigenvalues. This may be done in the spirit of the celebrated Anderson–Mott transition.[8–12] However, it is important to distinguish between the case where the "local perturbation" is included in the Hamiltonian describing the conduction band in the perfect crystal, and a second case, where this "local perturbation" is superimposed *in addition* to it (original Anderson model). While mathematically one may be able to move from one representation to the other, the origin of the perturbation appears to be of physical significance. For instance, one can base one's Hamiltonian on the "micro-classical" picture of nearest neighbor only pairwise interactions and a random distribution of vacancies and then easily show (for an infinite domain) that below the critical concentration all the eigenstates must be localized.[2,17,18] This is a case of a perturbation "internal" to the Hamiltonian (i.e., striking out all pairwise terms involving vacancies). While it is more difficult to tell what happens above the critical concentration, one assumes that one gets some infinitely extended eigenstates, in addition to several localized or pseudo-localized ones. However, in practice, we should realize that the addition to the Hamiltonian of even very small, long-range, pairwise interactions creates both practical and conceptual problems.[2,5] Obviously, as long as the range of the pairwise interactions is kept finite, one can always describe a "long-range" percolation topology,[5,16,18] giving a new critical percolation concentration. However, this concentration may be considerably lower than the experimental critical concentration, due to limitations such as finite excitation lifetimes (see below).

Even in the above case of nearest-neighbor only interactions, one may get zero transport for guest concentrations well *above* the critical percolation concentration. This may arise because of the discrete localized energy levels below the guest conduction band, which can trap out the excitons and restrict transport, provided that kT is small compared to the energy separation between the localized state and the delocalized band solutions.

If one adds to the above model small, but infinitely-long-range, interactions then it becomes intuitively obvious that some long range hops might occur between widely isolated "traps" (centers of localized states), even at very low temperatures, provided that one's time scale is unrestricted. In other words, given an infinite lifetime, the exciton will eventually visit every guest site, provided there is some interaction ("connectivity"). While the connectivity is always blocked, below the critical concentration, when restricted to short

range interactions, this is no longer true for "infinitely long range" interactions, no matter how small.

In molecular crystals there always exists some form of intermolecular long-range interaction, as well as a finite amount of thermal energy, kT. Also, any exciton, be it singlet or triplet, has a finite lifetime during which energy transfer may occur. The question thus becomes: Is the thermal energy large enough, or the lifetime of the exciton long enough, or the intermolecular interaction strong enough to expect long-range energy transfer. Obviously, for any given experimental system, the temperature is the only parameter of these three that can be varied. We will try to explain the temperature dependence of the energy transport in these systems. We note that recently the role of exciton-phonon coupling in localizing cluster states has been treated explicitly by Shinozuka and Toyozawa.[19]

We have used the naphthalene exciton systems (lowest singlet[5b] and triplet[5a]) to demonstrate exciton percolation. However, in past work, we have mainly used the singlet exciton for studying "static" percolation[20,18] and the triplet system for the study of "dynamic" percolation.[21,18] In the case of static percolation, the parameters of importance are the interaction topology and the guest concentration. It is treated similarly to the mathematical problem of two component site percolation and is similar to the "microclassical" model mentioned above, where the "vacancies" are now perdeuteronaphthalene. Here, the exciton lifetime is short enough so that a long-range hop involving tunneling and/or thermal activation takes a significant portion of the lifetime and thus is not a factor in percolation. In the dynamic percolation case, the excitation lifetime is involved explicitly; it is this lifetime τ that essentially defines the "connectivity." If, for instance, 10^3 exciton "hops" are required for the exciton to have an even chance of registering at a sensor (assuming a "hopping" model), then the average "jump time" is to be at most $10^{-3}\ \tau$, and this, in turn, defines the *maximal bond* between guest sites. It is this *maximal bond* that limits and defines the percolation topology. We have shown, for the triplet systems, that these "hops" are actually "exciton tunneling" (superexchange).[5a,22] Under appropriate conditions, exciton tunneling should be observable in the singlet exciton system as well. We demonstrate here that the same mechanism and superexchange approach can be utilized for both the singlet and the triplet exciton percolation. We thus get a unified description of exciton percolation in terms of a dynamic tunneling model with the temperature as the variable parameter. While the exciton tunneling itself, like any other exciton transfer mechanism, is basically a quantum mechanical manifestation, the percolation approach here is classical in the sense that a given bond is either "open" or "closed", based on the time consideration. Mathematically, we use a *long range percolation* approach.[16]

We have shown previously that efficient cluster-to-cluster exciton tunneling requires a thermal energy (kT) comparable to the spread in cluster energies.[5b] This is a simple activation energy requirement, somewhat similar to that for impurity band electron conduction. Thermal energy at 2 K is comparable to the difference in cluster triplet states for the naphthalene mixed crystal case. However, in the singlet case one has to elevate the temperature of the sample to about 4–10 K for this thermalization mechanism to become efficient. The present work involves a temperature dependence study of exciton percolation, both for the singlet and for the triplet case. Altogether, we compare five different systems (four triplet and one singlet) (see Table I) and find all of them to follow the same behavior, with no need of separately adjustable parameters. This is contrasted with a recent alternative interpretation[3] of our energy transfer data,[5] according to which the dependence of the exciton migration on the exciton carrier concentration is related to inhomogeneous broadening ("Anderson localization"). To summarize, we use throughout a cluster-percolation model, but emphasize that the definition of the clusters depends not only on static parameters (e.g. pairwise interactions), but also on "dynamic" parameters such as the excitation lifetime and the temperature.

TABLE I

List of systems

System	Host	Guest	$E_h - E_g$ (cm^{-1})	Supertraps (major)
I	$C_{10}D_8$	$C_{10}H_8$	88[a]	BMN[b]
II	$C_{10}D_8$	2-$DC_{10}H_7$	81[a]	$C_{10}H_8$
III	$C_{10}D_8$	1-$DC_{10}H_7$	72[a]	2-$DC_{10}H_7$; $C_{10}H_8$
IV	$C_{10}D_8$	1,4-$D_2C_{10}H_6$	57[a]	1-$DC_{10}H_7$; $C_{10}H_8$
V	$C_{10}D_8$	1,4,5,8-$D_4C_{10}H_4$	27[a]	1,4,5-$D_3C_{10}H_5$; 1,4-$D_2C_{10}H_6$

[a] The difference between the triplet host excitation energy (E_h) and guest energy (E_g) assumes a pure host (E_h is the bottom of the exciton band) and a highly dilute guest (E_g is isolated monomer energy). See Ref. 35.

[b] BMN is betamethylnaphthalene.

Experimental

The preparation and composition of the isotopic and chemical mixed crystals of naphthalene used in this temperature study has been previously published.[5,23] Table I lists the systems studied for the triplet exciton percolation analysis and a subset of this, System I, was involved in the singlet exciton temperature dependence studies.

The apparatus and procedures used in the emission experiments is the same as previously described with the following exceptions. The 1.2%,

4.7%, 9.9%, 17%, 35%, 45%, and 51% $C_{10}H_8$ samples were studied using an Air Products Model LT-3-110 variable temperature cryotip with the sample mounted as mentioned above. The temperature was monitored *via* a gold-chromel thermocouple embedded in the same piece of indium that the sample is in contact with. Several of the 5 K and 8 K spectra were taken using a Janis variable temperature dewar with the temperature measured by a calibrated carbon thermistor. All of the spectra at 1.7 K and 4.2 K were taken while the sample was in the immerson dewar. Further details pertaining to correlation of the various temperature dependent spectra to the three cryostats used, is given in Figures 6–12.

The long range exciton percolation model

If we accept the premise of the existence of a maximal bond range, based on time considerations,[16] it is self-consistent to argue that the condition (limit) of *supertransfer*[24] *percolation* applies as well. We recall that the maximal bond range n is actually a function of supertrap concentration, since the time allotted to each "jump" across a maximal bond was defined to allow for a succession of such jumps that would give an even chance for the exciton to register at a supertrap (this could include the contribution of the shorter bonds, which are both rarer and less time consuming[5a]). Thus, we assume that once the exciton has landed on a maxicluster it will register on a supertrap regardless of whether the maxicluster is a group of guests connected by nearest neighbor bonds or a group connected by "long range" bonds (including bondlengths from $n = 1$ to the maximal n). Therefore, we can use the very same formalism of percolation supertransfer that was developed for the short-bond problem.[24,25] Formally, the equation looks identical:

$$P = \bar{P}_\infty + \bar{C}_s I'_{av} \tag{1}$$

where P is the exciton percolation (registration) probability, $\bar{P}_\infty$ the site percolation probability (probability of the guest site being part of the guest maxicluster), I'_{av} the reduced average cluster size and $\bar{C}_s$ the "reduced" supertrap concentration (mole fraction of supertraps within the total guest site population, $\bar{C}_s \equiv C_s/C_g = Z/G$ where Z and G are the numbers of supertrap and guest sites, resp.). This formula can actually be replaced by a more rigorous one[24]

$$P = \sum_m \left[1 - \left(1 - \frac{m}{G}\right)^z\right] \frac{i_m m}{G} \tag{2}$$

where the improvement in rigor is singificant only in the vicinity of the critical guest concentration, C_c. We notice that P, $\bar{P}_\infty$ and I'_{av} are all functions of the guest mole fraction C_g and of the "topology". The topology is defined not only by the Bravais lattice (i.e. *square lattice*) but also by the *bond range* (e.g.,

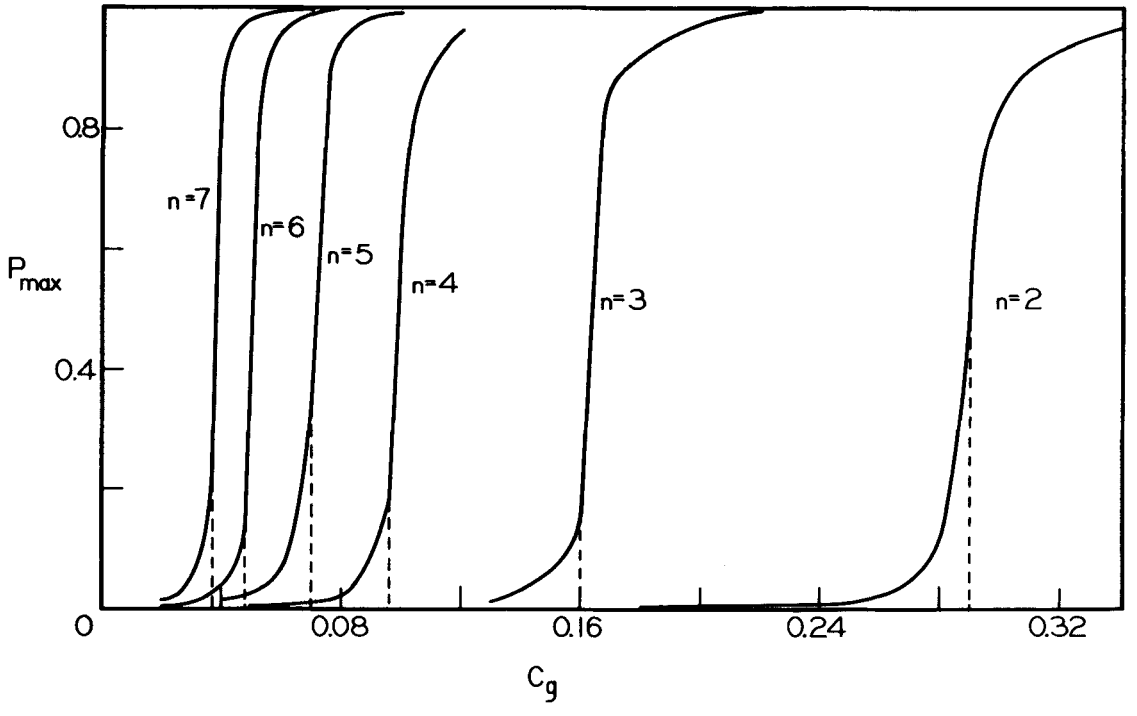

FIGURE 1 Comparison of the square lattice site percolation probability, P_{max} (probability of the guest site being part of the largest guest cluster) for different values of the long range percolation parameter n, as a function of the guest concentration C_g. Here, n is defined as the maximum number of nearest-neighbor bonds over which an interaction (or a connection) can occur. The function $\bar{P}_\infty$ (probability of a guest being included in an "infinite" cluster) is approximated by the dashed line from the P_{max} curve down to the calculated critical site concentration C_c^s below which $\bar{P}_\infty$ is zero, by definition.[15] All of the simulations for these curves were done for a square lattice of 500 × 500 sites. The effective coordination number is 12 for $n = 2$ and 112 for $n = 7$. For more details see Refs. 23 and 26. Note that a *universal* behavior has been demonstrated for all these n values: When P_{max} is plotted vs the *reduced* concentration $(C - C_c^s)/C_c^s$, the six curves do practically overlap in a linear representation,[53] as well as in a log–log representation[16] (giving a critical exponent[16] $\beta = 0.14$). Note that the $n = 1$ curve has been omitted as this is the well known $\bar{P}_\infty$ curve for the ordinary,[15] two-dimensional square lattice site percolation problem.

$n = 7$, meaning a maximal bond range defined by any succession of 7 nearest neighbor bonds).

The functions $\bar{P}_\infty$ have been derived for the *square lattice* for values $n = 1, \ldots, 7$, via techniques described elsewhere,[26] and are given in Figure 1. The functions I'_{av} for the same topologies have been given before.[5a] Thus using Eq. 1., we can plot P for the same topologies shown in Figures 2 for the value $C_s = 5 \times 10^{-4}$.

We can now take an empirical approach and argue that as long as the conditions for exciton tunneling are met, and when exciton tunneling is the dominant energy transfer mechanism, we expect the experimental data to fall on (or near) one of the theoretical curves in Figure 2. Thus, assuming an underlying square lattice topology for the exciton interactions (which has been justified elsewhere)[5] we can empirically determine the range n of the *effective* superexchange (tunneling) interaction. Since this effective interaction is defined by time considerations the range n does not have to be integral. However, in view of the experimental and theoretical uncertainties involved, the fractions in the values of n are of dubious significance. Looking at Figures 2 we can conclude that the experimental points correspond to a given $P(n)$ curve for the four triplet systems I–IV (in Table I) as well as system I in the singlet exciton case. It remains to be checked whether the respective values of n are consistent with the predictions of the exciton superexchange model for the respective systems.

THE CRITICAL TEMPERATURE FOR EXCITON PERCOLATION VIA TUNNELING

Percolation via tunneling involves cluster to cluster migration, where the connectivity of the clusters themselves maybe defined in terms of nearest neighbor bonds. Two clusters are rarely physically identical, except for monomers at low guest concentrations and where there is no environmental inhomogeneity. The sets of energy levels of two non-identical clusters are likewise non-identical. To conserve energy, the tunneling exciton has to either gain or lose the energy difference between its initial and final state. To avoid semantic difficulties we use the term *quasitunneling* for tunneling that involves the creation or annihilation of a phonon. Half the time, on the average, it involves annihilation, and is thus a *phonon assisted tunneling*. This requires a temperature $T > T_c$, where $kT_c \approx \delta/2.7$. Here δ is a weighted average of the range of energy differentials between the lowest energy levels of any two clusters involved. This idea has been discussed before[5] for both triplet and singlet naphthalene excitons. It has been argued qualitatively[5,18] that for the

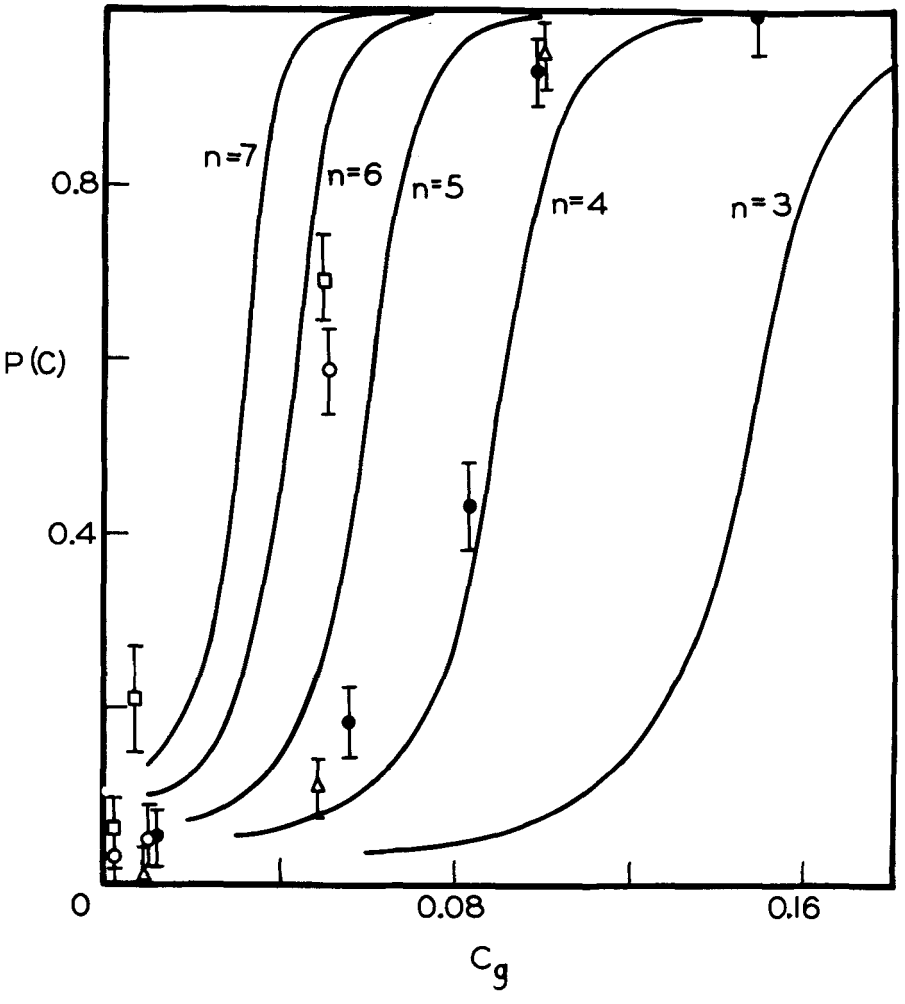

FIGURE 2a The exciton percolation probability $P(C)$ as a function of guest concentration (with the interaction range n as parameter for the theoretical curves). The *theoretical* curve is *calculated* from the cluster model of exciton migration, i.e., Eq. 2. We have assumed a constant supertrap concentration $C_s\,(= ZC/G) = 5 \times 10^{-4}$. We note that this formula is based on the "supertransfer" assumption[4,37] for dynamic percolation (i.e., time dependent connectivity).

The experimental points represent the normalized emission intensities[5,23] I_s/I_{total}, for the four triplet systems in Table I, where s designates the supertrap. These are based on some minor refinements[23] of the data in Table II with System I represented by solid circles, System II by triangles, System III by squares and System IV by open circles. The relative concentrations of trap/supertrap and the experimental conditions are given in Ref. 5.

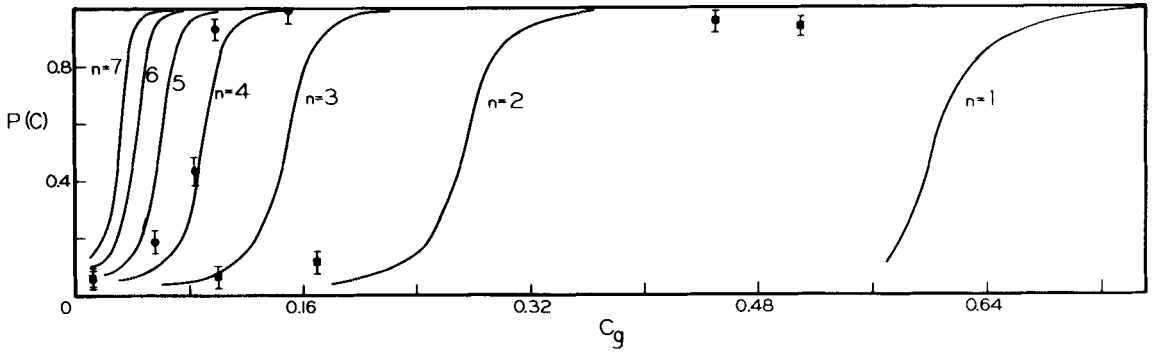

FIGURE 2b Calculated and experimental exciton percolation data comparing the singlet exciton to that of the triplet exciton state for System I ($C_{10}H_8/C_{10}D_8$). The triplet data (circles) are at 1.8 K while the singlet data (squares) are at 8 K to ensure dynamic percolation.[23] The sensor is beta-methylnaphthalene, at a concentration of about 10^{-3} throughout.[23] We use the expression $P(C) = I_S/I_{total}$ where I_s is the sensor luminescence and I_{total} is the normalized[23] total emission (sensor plus $C_{10}H_8$). The theoretical $P(C)$ is derived and plotted in the same manner as in Figure 2a. The point at $C_g = 0.05$ is for $T = 10$ K and thus exhibits a high $P(C)$ value.

naphthalene triplet excitons $T_c \approx 1.5$ K, while for the lowest singlet, $T_c \approx$ 20 K. More precisely, one should arrive at T_c in the following way:

1) Determine the dynamic (tunneling) critical percolation concentration C_c.

2) Consult cluster distribution tables to determine which are the predominant clusters at this concentration.

3) Determine the "typical" energy spread δ for the predominant clusters, assuming that, for the most part, the lowest energy levels of the cluster have the highest population probability.

Alternatively to steps 2 and 3, the spectral distribution of cluster emission can be analyzed to yield the same sort of information.

For the singlet exciton case, it is reasonable to assume δ to be about a quarter of the pairwise interactions (i.e. $\sim 5\ \text{cm}^{-1}$). This is based on cluster distributions[2,27] and their corresponding energy levels, for $C_g \approx 0.30$. Thus, $T_c \approx 10$ K. For the triplet case, only monomers, dimers and trimers need be considered for guest concentrations up to 10%. This leads to $\delta \approx 0.5$–$1\ \text{cm}^{-1}$ or $T \approx 1$ K. However, we notice in the triplet emission spectra, at guest mole fractions around 0.08, a naphthalene-d_8 "defect state"[28] at about $8\ \text{cm}^{-1}$ lower in energy than the "normal" naphthalene-h_8 component (see Figures 39 and 40). The defect site can be classified as either a supertrap or trap depending upon the temperature domain of the system. When $kT \ll 8\ \text{cm}^{-1}$, then the defect behaves as a supertrap. When $kT \approx 8\ \text{cm}^{-1}$, then most excitons that are trapped by the defect sites are able to "boil out" into the guest sublattice. Because of the low C_s of the X-trap, $T_c \approx 4$ K. For the three other triplet systems in this study (see Table II), one needs only to take into account

TABLE II

Comparison of experimental and theoretical percolation concentrations ($\bar{n}$ is based on Eq. 6, with $\beta = 1.25\ \text{cm}^{-1}$; n (exper.) on interpolation, Figure 2a)

System	n (exper.)	C_g(exper.)[23] (mole fraction)	$\bar{C}_s$	$\frac{\sigma}{\gamma_{t-s}}$	Δ (cm^{-1})	$\bar{n}$	τ_g sec	$C_c^s(\bar{n})$ (mole fraction)
I	4.3	0.085 ± 0.02	0.003	100	93	4.9	2.5[a]	0.073
II	4.4	0.07 ± 0.02	0.03	100	86	5.7	2.6[b]	0.055
III	5.6	0.03 ± 0.02	0.09	100	77	6.3	3.0[c]	0.046
IV	5.8	0.04 ± 0.01	0.04	100	62	6.4	3.65[d]	0.043

[a] M. A. El-Sayed, M. T. Wauk, and G. W. Robinson, *Mol. Phys.*, **5**, 205 (1962).

[b] N. Hirota and C. A. Hutchison, *J. Chem. Phys.*, **46**, 1561 (1967); measurement in durene and durene-d_{14} at 77 K.

[c] R. J. Watts and S. J. Strickler, *J. Chem. Phys.*, **49**, 3867 (1968).

[d] T. D. Gierke, R. J. Watts, and S. J. Strickler, *J. Chem. Phys.*, **50**, 5425 (1969). This value is an average of 3-methylpentane and ethanol solvent (glasses) values at 77 K.

monomers and dimers, thus giving $\delta \approx 1\ \text{cm}^{-1}$ and $T_c \approx 1.5$ K, just about our lowest temperature (~ 1.6 K). Obviously, one has to avoid temperatures high enough to cause phonon assisted thermalization from the guest cluster into the host band, thus bypassing the process of exciton tunneling or percolation. The conditions for such a thermalization are discussed further below.

SUPEREXCHANGE AND TUNNELING INTERACTIONS

The basic considerations involved in the triplet exciton tunneling have been discussed before.[5,18,21] The major exciton pairwise interactions in the lowest triplet state of naphthalene are the *four* nearest neighbor, interchange equivalent, pairwise exciton interactions between a molecule at the origin and another molecule at $\pm\frac{1}{2}(a \pm b)$, i.e., in the *ab* plane (see Figure 3). This interaction has been given by Hanson[29] (and recently by Port *et al.*[30]) as $1.25\ (\pm 0.05)\ \text{cm}^{-1}$. The next nearest interaction is *also* in the *ab* plane, and is about[29–31] $0.5\ \text{cm}^{-1}$. The out-of-plane interactions are orders of magnitude smaller.[32] It thus turns out that for the purposes of tunneling (superexchange) calculations, the major contribution comes from the nearest neighbor, interchange equivalent interaction. This interaction is not only more than twice as large as the next one but (being "interchange equivalent") has also a significantly larger "coordination" number, *four* [along $\pm\frac{1}{2}(a \pm b)$], compared to only *two* for a translationally equivalent interaction (i.e., along the *a* or *b* axis). Thus, the general tunneling interaction[5,33] can be expressed as:

$$J_{\bar{n}} = \frac{\bar{\Gamma}_{\bar{n}}\beta^{\bar{n}}}{\Delta^{\bar{n}-1}} \tag{3}$$

where $J_{\bar{n}}$ is the superexchange interaction between two guest molecules separated by a minimal succession of $\bar{n}$ nearest neighbor bonds (passing through $\bar{n} - 1$ host sites), β is the pairwise direct interaction (here $1.25\ \text{cm}^{-1}$) and Δ is the guest-host trap-depth, i.e., the energy separation in the ideal mixed crystal[34] (e.g. $93\ \text{cm}^{-1}$ for system I[35]). $\bar{\Gamma}_{\bar{n}}$ is the *average number of routes*,[5,33] involving $\bar{n}$ short bonds, between the two guest sites. The "jump time" of an exciton, from one guest site to another[5] is about[36]

$$t_j \approx (2J_{\bar{n}})^{-1} \tag{4}$$

where J is in units of Hz and we have assumed that each guest site in the mixed crystal is connected with an average of *two* nearest guest neighbors. The average time for reaching a supertrap, with a supertrap over guest mole fraction of $\bar{C}_s$, is thus:[5,23]

$$t = \frac{\sigma}{\gamma_{t-s}\bar{C}_s t_j^{-1}} = \frac{\sigma\Delta^{n-1}}{2\bar{C}_s\gamma_{t-s}\bar{\Gamma}_{\bar{n}}\beta^{\bar{n}}} \tag{5}$$

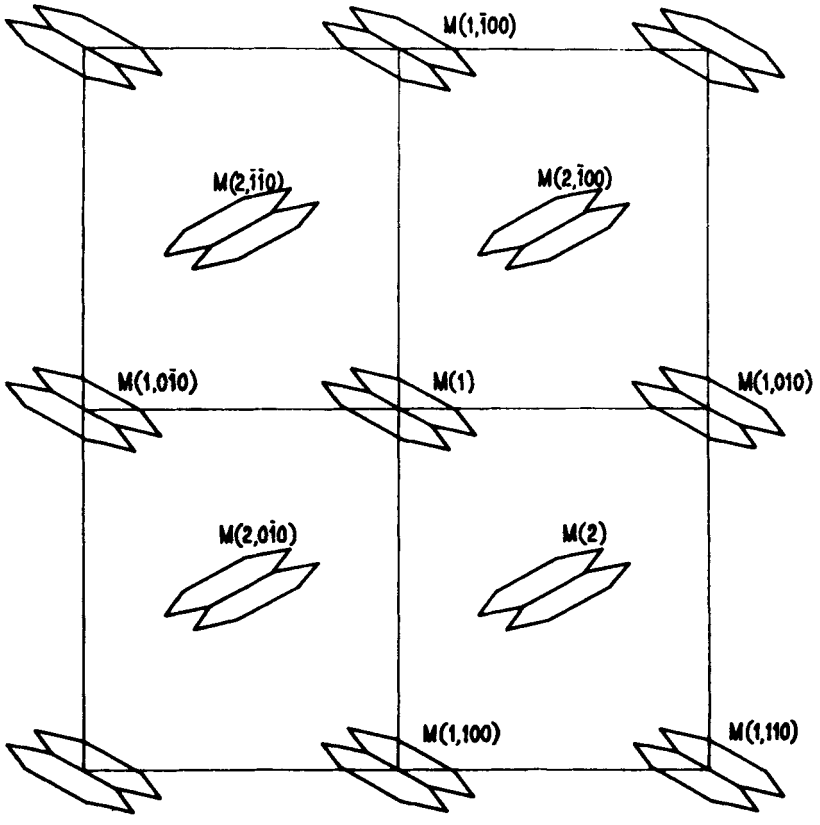

FIGURE 3 Crystallographic projection of the naphthalene structure along (001) on the (*ab*) plane. The molecule of reference is labeled $M(1)$. All of the translationally equivalent sites are denoted $M(1, hk1)$ while all of the interchange equivalent sites are $M(2, hk1)$. This projection is from Hartmann.[63] The axis perpendicular to it is defined as c'.

or

$$t = \frac{\sigma \Delta^{\bar{n}-1} C_g}{2C_s \gamma_{t-s} \bar{\Gamma}_{\bar{n}} \beta^n} \leq \tau_g \tag{6}$$

where γ_{t-s} is the trap-supertrap trapping efficiency[5,23] and σ is the average number of jumps required per visit of a distinct site. Our guesstimate of the value of γ_{ts} is about $\frac{1}{2}$ for these triplet systems[5,23] and about[23] 50 for that of σ. Note that σ is an order of magnitude larger here than for the case of a simple random walk on a square lattice. There are two reasons for the difference. First, the visitation efficiency on a binary random lattice (with a high concentration of "blocked" sites) is significantly reduced,[37] compared to a perfect lattice. In addition, "long-bond" jumps seem to further reduce this

efficiency.[38] Also, we include in this factor the effects of phonon assistance (see below), as we do in γ_{ts}. Thus σ/γ_{ts} is temperature dependent. The estimates above give us a value of 10^2 for the factor σ/γ_{ts}. If we set the elapsed time t equal to the lifetime[5,28] $\tau \approx 2.5$ sec, one can solve for the value of $\bar{n}$ as a function of $\bar{C}_s$. While the above values of the parameters τ and Δ were specific for our system I (see Tables I, II) similar, known values are avilable for the systems II, III and IV (Table II). We note here that the values of $\bar{C}_s$ are approximate, and that $\bar{C}_s$ of system I varies over an order of magnitude or more.[5,23]

Utilizing Eq. 6 for several values of C_s, we can plot the effective tunneling range necessary to give a total tunneling time of 2.5 seconds for each guest concentration studied. In other words, if we set $t = \tau_g = 2.5$ sec and solve Eq. 6 for n, we get the two curves shown in Figure 4. In addition to the curves from Eq. 5 we superimpose the $S_{\max}$ ($\equiv n$) *vs.* C_c^s curve for two dimensions from reference.[16] For each value of C_g, along a curve of constant C_s, there will be a corresponding required interaction length n^*, where the tunneling time will total 2.5 sec. The next step is to examine the C_c^s *vs.* n curve and find at what percolation concentration, C_c^s, is the average tunneling length n^* bonds. This value for C_c^s should be compared to the nominal C_g of the sample. If $C_c^s > C_g$, then the guest sites in the sample of C_g are farther apart than n^* bonds, $\bar{n} > n^*$, and the exciton will not be able to complete all the tunneling through $\bar{n} - 1$ host sites necessary to percolate. If $C_c^s < C_g$ that means that the longest *possible* "jump," n^*, is longer than $\bar{n}$, which is the maximum length of jump found in the extended long range cluster. In other words, jumps of n^* are possible but only jumps of $\bar{n}$ are necessary. Thus, the exciton should find a supertrap within 2.5 sec. Stated simply, if a point in Figure 4 is above the $S_{\max}$ *vs.* S_c^s curve, then a sensor should be found within 2.5 sec, if it is below the $S_{\max}$ *vs.* C_c^s curve then the lifetime is too short for a sensor to be found. C_g^* is the crossing point of the constant C_s curve with the $S_{\max}$ *vs.* C_c^s curve. It is the concentration threshold where trap-trap or cluster-cluster tunneling becomes important. If we assume that, in the triplet state, the splitting $\delta_{m-m'}$ between the energy levels of different size guest clusters is comparable or small relative to kT at 1.7 K, then there will be no localized cluster states to compete with the sensor for the exciton. For the $^3B_{1u}$ exciton in naphthalene, this is practically the case. (There is still an effect on the kinetics, which is further discussed below and elsewhere[28]). If we look closely at Figure 4 we see that the value for C_g^* is somewhere between 6.2 and 7.8% guest concentration, depending upon the choice of C_s, which ranges between 0·1 and 0·01% supertrap. Again this assumes that the ratio of $\sigma/\gamma_{t-s} \simeq 100$ in these fairly dilute mixed crystals. (Obviously decreasing this factor by ten has the same small effect as increasing C_s by a factor of ten).

It should be noted that without the mathematical solution to the long-range percolation problem[16,39,40] we would not be able to perform the above test or even rationalize our data quantitatively. The C_c^s *vs.* n curve

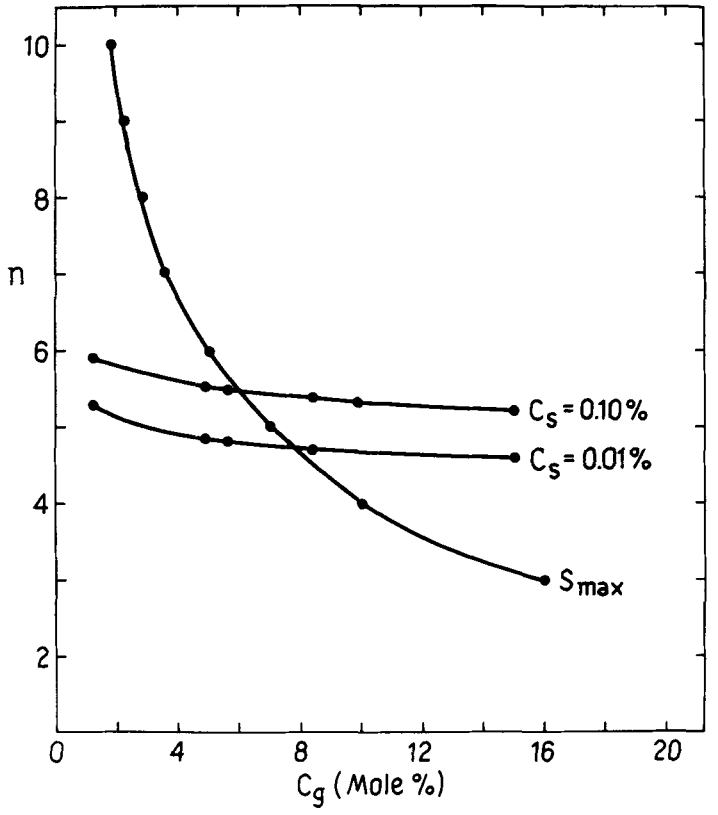

FIGURE 4 Interaction range n vs. C_g for superexchange tunneling of the $C_{10}H_8$ $^3B_{1u}$ exciton. The two curves with C_s as a parameter have been calculated from Eq. 6 where β, along $\pm\frac{1}{2}(a \pm b)$, is the only pairwise interaction considered, and where we have set $t = \tau_g = 2.5$ sec and have solved Eq. 6 for n as a function of C_g. From these curves one is able to find the maximum range of interaction necessary for an exciton to be trapped by a sensor within its lifetime at any given guest concentration. In addition to these curves, the dependence of two-dimensional C_c^s, the critical percolation concentration, on the range of interaction has been superimposed. This relationship is the curve from reference 16 where $n \equiv S_{max}$.

(S_{max}) is the necessary "dictionary", relating the optimum superexchange range $\bar{n}$ with the critical percolation concentration $C_c(\bar{n})$, the only underlying assumption being that of a *square lattice* interaction topology.

We can now apply the above method of analysis to the singlet exciton of system I. We show elsewhere[23] that for the singlet system, in the typical tunneling range ($0.1 \leq C_g \leq 0.4$), we can use the simple Eq. 6, where the superexchange is based only on the nearest neighbor direct pairwise interactions, $\pm\frac{1}{2}(a \pm b)$, even though there are significant translational interactions not only in the *ab* plane but also between such planes.[22,41] The nearest neighbor (interchange equivalent) direct pairwise interaction is about[22,41]

$18\ cm^{-1}$, while the translational interactions *in* and *out-of-plane* are a factor of 2 to 3 smaller. It is only in the low concentration region of the tunneling range ($0.01 \leq C_g \leq 0.1$), where the latter interactions become important. Moreover, at the lower end of this last concentration range, the very long-range, direct transition-dipole exciton exchange interactions become significant.[23] However, here we only discuss the tunneling percolation region, where the longer range direct interactions contribute little. If we simply substitute into Eq. 5, using a trapdepth[42] of $115\ cm^{-1}$, $C_s = 10^{-3}$, $\sigma/\gamma = 50$ (reducing σ, due to higher C_g) and a life-time[43] of 100 ns, we calculate $\bar{n} \approx 2.8$.

The calculated curve in Figure 5 gives for a sample of 10^{-3} supertrap and guest concentration C_g the value n^* or the "average" tunnel length necessary

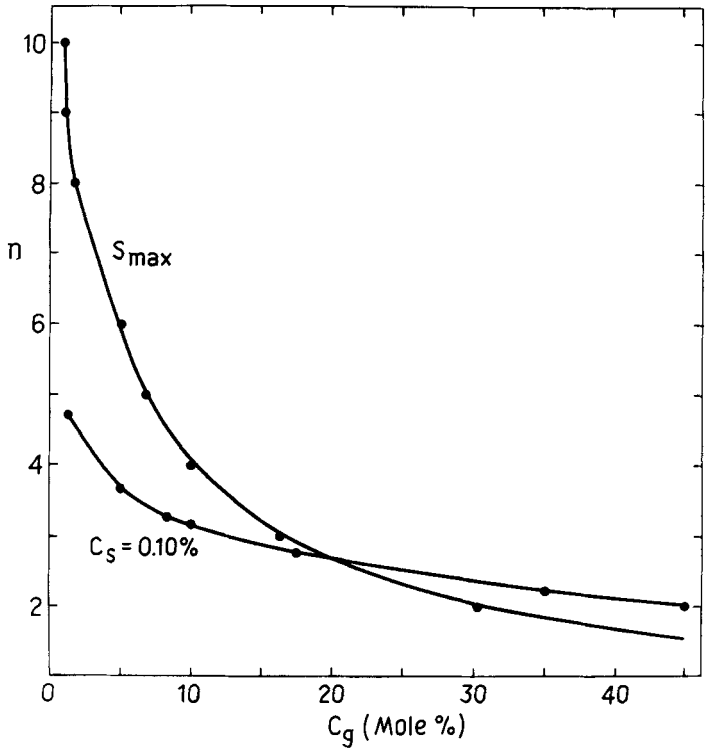

FIGURE 5 Interaction range n vs. C_g for superexchange tunneling of the $C_{10}H_8$ $^1B_{2u}$ exciton. This figure is identical in concept to Figure 4. The assumption made here, as in Figure 4 is that $\delta_{m,m'} \leq kT$. The curve where $C_s = 0.10\%$ has been calculated from Eq. 6 with the appropriate values for Δ, β, and σ (see text). Only pairwise interactions along $\pm\frac{1}{2}(a \pm b)$ have been considered for these heavily doped mixed crystals. We have set $t = \tau_g = 100$ nsec and have solved Eq. 6, for n as a function of C_g. From this curve one is able to find the "maximum" range of interaction necessary for an exciton to be trapped by a sensor within 100 nsec at a given guest concentration. In addition to this curve, the dependence of the two-dimensional C_c^s, critical site percolation concentration, on the range of interaction has been superimposed.

to find a supertrap within the 100 nsec lifetime. We can also see that, for a supertrap concentration of $\simeq 10^{-3}$, the guest concentration at which the n^* *vs.* C_g curve intersects the S_{max} *vs.* C_c^s curve is $\simeq 18\%$. We defined this concentration as C_g^*. (We note that this calculation excludes any temperature dependent factors related to phonon-assisted activation, unless incorporated in the "fudge factor" σ/γ). Thus, for a constant C_s, if $C_g < C_g^*$ there will not be efficient tunneling among the different clusters and hence no dynamic percolation. Only when $C_g > C_g^*$ for a given sensor concentration, will the average tunnel length $\bar{n}$, at C_g, be shorter than that necessary to find a supertrap in 100 nsec or less, *i.e.*, less than n^*. Thus C_g^* should be the guest concentration where cluster-cluster tunneling becomes important, assuming that $kT \simeq \delta$.

The treatment of the triplet exciton's tunneling is simplified by the relatively small nearest neighbor interaction, 1.25 cm^{-1}. The effect of this is to make δ comparable or small relative to kT even at 2 K. However, in the case of the $^1B_{2u}$ exciton, δ is not always small compared to kT. Thus not all of the cluster states are populated at low temperatures and there may exist localized cluster states[2,5] even for an infinitely extended cluster (e.g. one monomer and an infinite chain of dimers loosely bound by longer range interactions). If a fraction of the states are "localized" and unpopulated due to a small value of kT, then one should use the effective guest concentration C_g', which represents the fraction of guest giving rise to the "delocalized" states that are available for cluster-cluster tunneling by the above-mentioned formalism (e.g. in the above example omit the monomer). If $C_g < C_g^*$ then no amount of kT will promote cluster-cluster tunneling, only transfer due to guest-host thermalization will occur. If $C_g > C_g^*$ then the temperature has to be raised to a point where $C_g' \simeq C_g^*$ and then tunneling will occur. It should be noted that the localized cluster states may still contribute to the guest emission, and this fraction of the total guest should be calculated from a table[44] of (nearest neighbor) monomer, dimer, trimer and tetramer probabilities since some of these smaller clusters may be mostly responsible for the localized states. In summary, we can use Eq. (6), and the accompanying formalisms, to calculate the extent of long-range exciton tunneling. We predict extensive cluster-cluster tunneling when the guest concentration $C_g > C_g^*$, if $kT \geq \delta$. In the low temperature limit, *i.e.*, $kT \leq \delta$, we predict long range exciton transport only when $C_g' > C_g^*$.

HOST BAND THERMALIZATION VS. PERCOLATION

There are basically two mechanisms by which an exciton that is localized in a guest cluster can communicate with other guest clusters. One way is the thermal detrapping from the guest cluster into the host band and then back

into another guest cluster. The other can be described as direct trap-trap transfer *via* either the above discussed superexchange tunneling or direct long range (*i.e.*, dipole-dipole) interactions as described elsewhere.[23] In our present ternary system, the extent to which either or both of these mechanisms occur is reflected in the relative emission emanating from the BMN supertrap compared to that from the $C_{10}H_8$ trap species. The phonon-assisted thermal depopulation of the guest excitons to the host band is strongly temperature dependent and is proportional to the Boltzmann factor $\exp[(E_h - E_t)/kT]$ where $E_h - E_t$ is the energy from the trap cluster to the bottom of the host band, which is at least $50\,cm^{-1}$ for the $C_{10}H_8/C_{10}D_8$ singlet system,[2,45] and e.g. $88\,cm^{-1}$ (Table I) for the triplet system [Note that the "trap" (t) means practically the same as "guest" (g)].

To focus our attention on the trap-host-trap mechanism of energy transfer we look at the dilute guest region. In the 1.2% guest sample we can study the thermalization from the guest monomers and dimers into the host band with increasing temperature, free from the interference of any *extensive* trap-trap tunneling, for both the singlet[23] and triplet.[28] Thus the thermalization into the host band is the primary mechanism of temperature-assisted trap-to-trap transfer, at these low guest concentrations.

In the limit of low illumination and rapid excitation transport (relative to lifetime), the steady state emission from the BMN and $C_{10}H_8$ will achieve a value representing excited state "thermal equilibrium":

$$\frac{I_t}{I_s} = \frac{K_t}{K_s}\frac{C_t}{C_s}e^{-\Delta'/kT}, \tag{7}$$

where Δ' is the difference in energy between the trap and the supertrap ($\simeq 476\,cm^{-1}$ singlet, 240 triplet) and K_s and K_t are the radiative yields (quantum efficiencies corrected by spectral window Franck–Condon factors). With this large value for Δ', it is plain to see that the "equilibrium" value of I_t/I_s is about zero for the low temperatures that we studied (< 30 K). However, our system is rate limited, due to a slow exciton transport. It simply takes time to repeatedly thermalize the exciton out of the isolated traps into the *host* band until it is eventually trapped out by a supertrap, from which no thermalization occurs. Thus the normalized intensity ratio will depend upon both the transfer rate k_{transfer} (time averaged) and the overall decay rate k_{decay}. Assuming that, initially, only the traps were excited and not the supertraps:

$$\frac{I_s}{I_t}[\alpha\bar{C}_s]^{-1} = \frac{k_{\text{transfer}}}{k_{\text{decay}}}$$

$$= \frac{\tau_t}{t_{\text{transfer}}} \tag{8}$$

Here, τ_t is the lifetime of the trap species, $\alpha = K_s/K_t(\gamma_s/\gamma_t)$ where γ is a trapping efficiency and t_{transfer} is defined as:

$$t_{\text{transfer}} = t_j \frac{\exp[(E_h - E_t)/kT]}{F'} + t_{\text{host}} \tag{9}$$

where F' is a modified Franck–Condon factor which deals with the overlap of the phonon density-of-states necessary for phonon assisted thermalization into the host band. The quantity t_j is the jump time from the trap to the host site as $(E_h - E_t) \to 0$. The quantity t_{host} is the time that it takes for the exciton, once in the host band, to be trapped out by another guest site. We assume that in the limit of super-transfer[18] t_{host} is negligible compared to the first term in Eq. 9. If we substitute Eq. 9, neglecting t_{host}, into Eq. 8, we get:

$$\frac{I_s}{I_t} = \frac{C_s \tau_t \alpha F'}{C_t t_j} \exp\left[- \frac{E_h - E_t}{kT} \right], \tag{10}$$

which relates the emission intensity ratio to the temperature. If we were to increase the temperature by an order of magnitude (from 1.7 to 17 K), we would expect an increase in I_s/I_t of $\exp[-50/13]/\exp[-50/1.3] \simeq 10^{15}$, in the dilute mixed crystal limit (for the singlet).

If we want to distinguish thermally assisted trap-trap and trap-supertrap transfer from the thermalization into the host band, we have to look at the more heavily doped crystals. As the concentration of guest sites is increased, the guest cluster distribution changes, as was discussed before.[2,5b] It is well known that if we increase the guest concentration, we progress from the isolated monomer state (close to the center of the guest exciton band) to larger and larger cluster states. Finally we reach the pure guest states. Thus the position of the lowest $^1B_{2u}$ exciton state decreases steadily in energy (until it reaches the pure guest band edge which is about the same as the lower Davydov component).[17] This makes for reduced thermalization into the host, but enables guest-guest transfer. The guest-guest (cluster-cluster) thermalization is characterized by a factor $\exp(-\delta/kT)$, as mentioned before, where δ is the energy difference between the lower lying "donor cluster" (m) energy level and the higher lying "acceptor cluster" (m') energy level.

Having looked at the two extreme conditions where, in each case, only one of the two competing mechanisms is of primary importance, let us now predict what should happen at intermediate concentrations and temperatures. We then can compare our experimental results to the above simple formalism.

In order to predict the $^1B_{2u}$ exciton's behavior in dilute mixed crystals, we now refer back to Eq. 10. If we were to experimentally determine the

temperature for each sample C_g where $I_s/I_t = 1$, we could then write, using Eq. 10,

$$C_t = \left[\frac{\alpha C_s \tau_t F'}{t_j}\right] \exp\left[-\frac{E_h - E_t}{kT}\right]. \tag{11}$$

If we then take the natural logarithm of both sides we get:

$$\ln C_t = \ln B - \frac{(E_h - E_t)}{k}\frac{1}{T} \tag{12}$$

where we have assumed a constant C_s and defined the intercept B as:

$$B = \frac{\alpha C_s \tau_t F'}{t_j}. \tag{13}$$

Thus, if we plot the $[T]^{-1}$, at which $I_s/I_t = 1$, for each experimental point, *versus* $\ln C_t$, we would expect to get a straight line for as long as the host thermalization mechanism was dominant. This should apply in the dilute guest limit. At higher guest concentrations, the value of the temperature at which point $I_s = I_t$ is strongly dependent upon the guest concentration, since the concentration determines the cluster distribution and therefore which δ values will be important. In other words, the *temperature* determines the value of C_g'. The quantity δ enters as an exponential term $\exp[-\delta_{m,m'}/kT]$, so that we expect a *strong* exponential-like dependence of I_s/I_t on T *as well as* C_g, for the more heavily doped samples. At intermediate concentrations, both mechanisms will be involved, to one extent or another. We thus expect the actual experimental curve to be a superposition of the dilute case (C_g independent) behavior and the heavily doped (C_g dependent) behavior. We would expect to see a break-point or knee in the curve around the concentration where there is a crossover from one dominant mechanism to another.

Figures 6–12 show the BMN origin *vs.* the $C_{10}H_8$ "510" vibronic *fluorescence* band for seven guest concentrations as a function of temperature. At 1.7 K, $I_{C_{10}H_8} \gg I_{BMN}$ for the entire concentration range (1.2–51%). As the temperature is increased, a point is reached where the BMN and the $C_{10}H_8$ emission are equal in intensity, and as the temperature is further elevated, an increasing amount of emission emanates from the supertrap species. In Figure 13 we plot the inverse of *the temperature, at which the BMN intensity about equals the* $C_{10}H_8$ *intensity* for each sample, *versus* $\ln C_g$. We see that, indeed, the temperature where $I_{BMN} \simeq I_{C_{10}H_8}$ decreases sharply, after a point, as the concentration increases. As the temperature is raised, kT becomes comparable to δ; and thus C_g', the effective guest concentration, approaches the nominal guest concentration. The expected "knee" is observed around 20%.

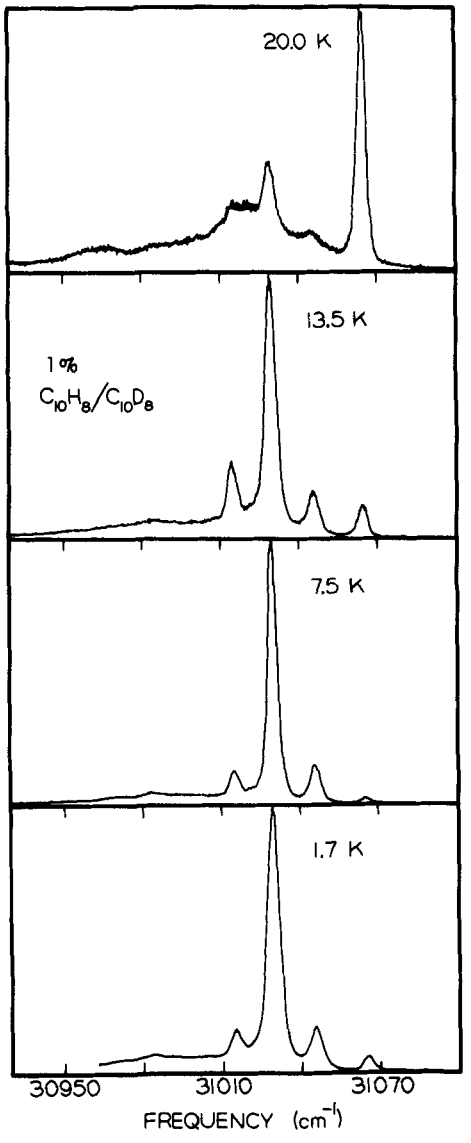

FIGURE 6 Temperature dependent dynamic $^1B_{2u}$ percolation for the 1.2% guest sample. The $C_{10}H_8$ 0-"510" cm^{-1} vibronic band at $\simeq$31,030 cm^{-1} is compared to the intensity of the BMN 0—0 band at 31,064 cm^{-1}. The 1.7 K spectra was taken while the sample was immersed in liquid He while those at 7.5, 13.5 and 20 K were taken in an Air Products variable temperature cryotip. Note that the peak at 31,015 cm^{-1} for the 20 K spectrum is a BMN phonon sideband.

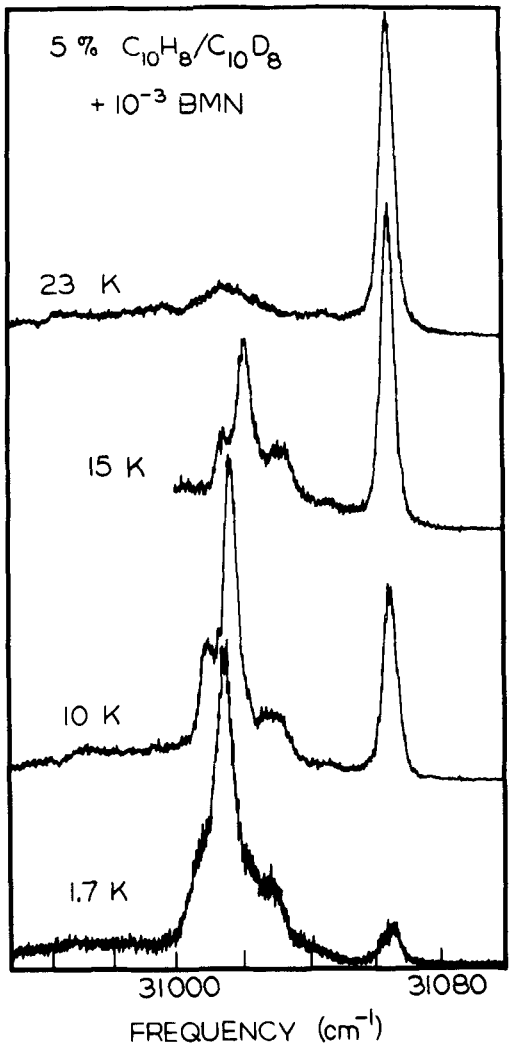

FIGURE 7 Temperature dependent dynamic $^1B_{2u}$ exciton percolation for the 5% guest sample. The $C_{10}H_8$ 0-"510" cm^{-1} vibronic band at $\simeq$31,020 cm^{-1} is compared to the intensity of the BMN 0—0 band at 31,064 cm^{-1}. The 1.7 K spectra was taken while the sample was immersed in liquid He, while the 10, 15, and 23 K spectra were taken in an Air Products variable temperature cryotip. Note the shift to higher energy of the $C_{10}H_8$ band as the temperature is increased, due to enhanced emission from the smaller clusters with higher energy states which are made more accessible by the increased kT. There is also a temperature dependent shift to higher energy for all the individual cluster states which is *much* stronger in $C_{10}H_8$ than in BMN.[64] Note also that the peak at $\simeq$31,015 cm^{-1} in the 23 K spectrum is a BMN phonon sideband, not residual $C_{10}H_8$ emission.

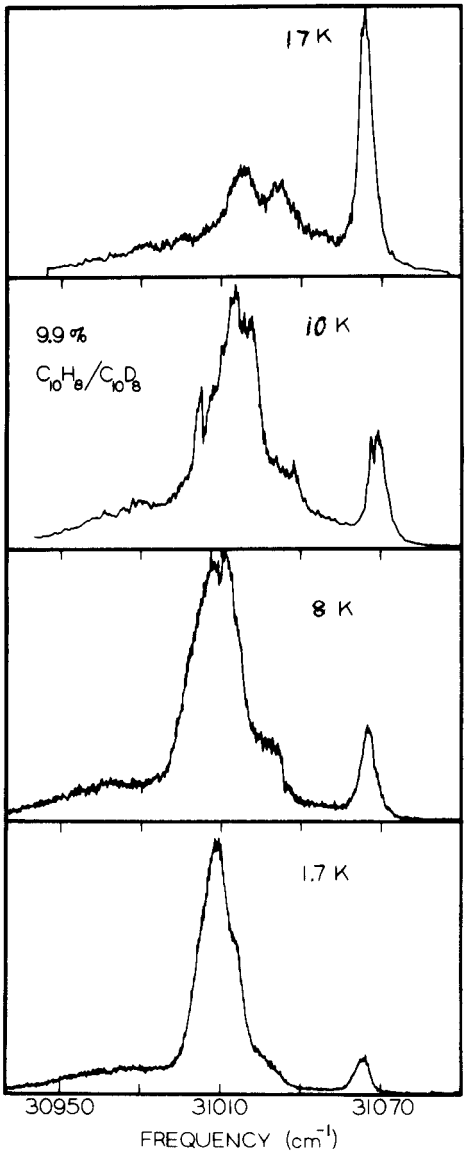

FIGURE 8 Temperature dependent dynamic $^1B_{2u}$ exciton percolation for the 9.9% guest sample. The $C_{10}H_8$ 0-"510" cm^{-1} vibronic band at $\simeq$31,015 cm^{-1} is compared to the intensity of the BMN 0—0 band at 31,064 cm^{-1}. The 1.7 K spectra was taken while the sample was immersed in liquid He, while the 8, 10, and 17 K spectra were taken in an Air Products variable temperature cryotip. The spike on the low energy side of the $C_{10}H_8$ band at 10 K is a change in the Xe arc lamp intensity. Note the shift to higher energy of the $C_{10}H_8$ band as the temperature is increased due to the enhanced emission from the smaller clusters with higher energy states which are made more accessible by the increased kT. Note that the peak at $\simeq$31,015 cm^{-1} in the 17 K spectra is a BMN phonon sideband.

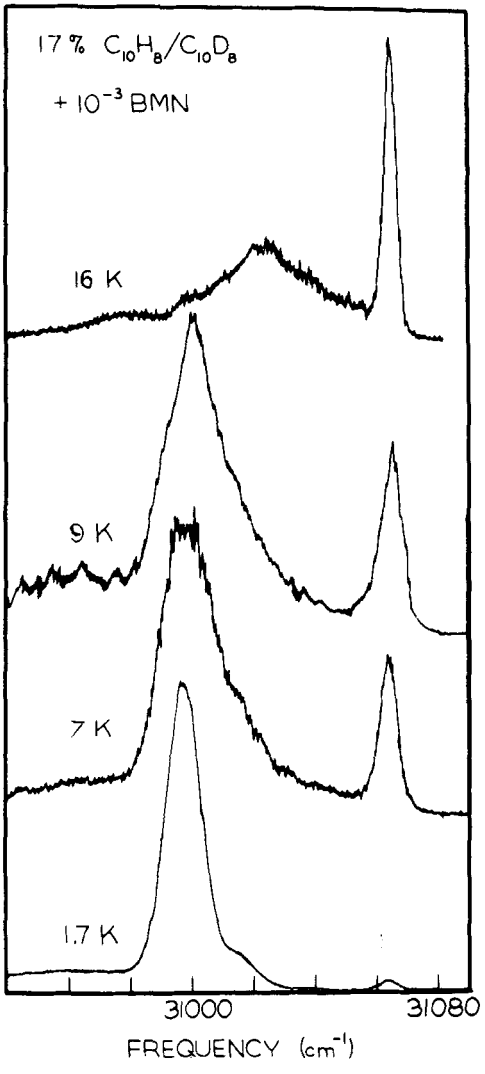

FIGURE 9 Temperature dependent dynamic $^1B_{2u}$ exciton percolation for the 17% guest sample. The $C_{10}H_8$ 0-"510" vibronic band at $\simeq$31,000 cm^{-1} is compared in intensity to the BMN 0—0 band at 31,064 cm^{-1}. The 1.7 K spectrum was taken while the sample was immersed in liquid He, while the 7, 9 and 16 K spectra were taken in an Air Products variable temperature cryotip. Note that the peak at $\simeq$31,020 cm^{-1} in the 16 K spectrum is a BMN phonon sideband.

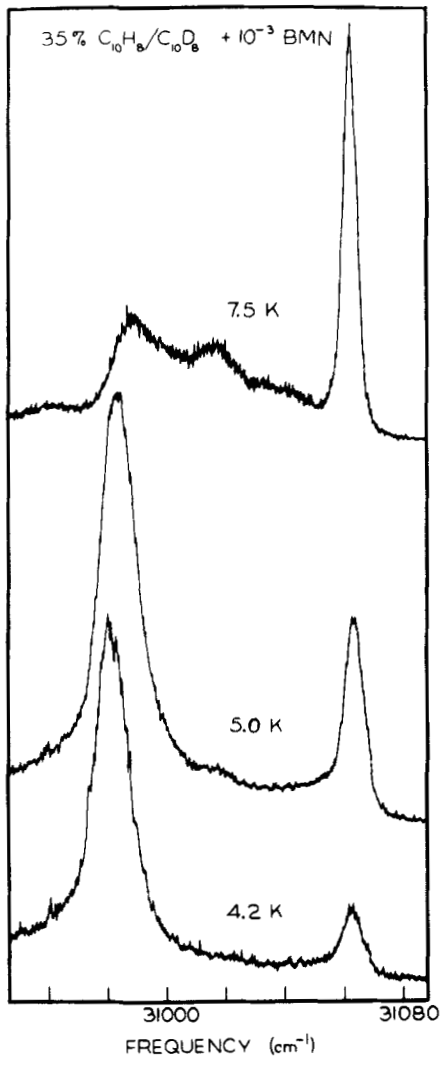

FIGURE 10 Temperature dependent dynamic $^1B_{2u}$ exciton percolation for the 35% guest sample. The $C_{10}H_8$ 0-"510" vibronic band at $\simeq$30,985 cm^{-1} is compared to the intensity of the BMN 0—0 band at 31,063 cm^{-1}. The 4.2 K spectrum was taken while the sample was immersed in liquid He, while the 7.5 K spectrum was taken in an Air Products variable temperature cryotip. The 5.0 K spectrum was taken in a Janis variable temperature dewar. Note that the peak at $\simeq$31,015 cm^{-1} in the 7.5 K spectrum is a BMN phonon sideband.

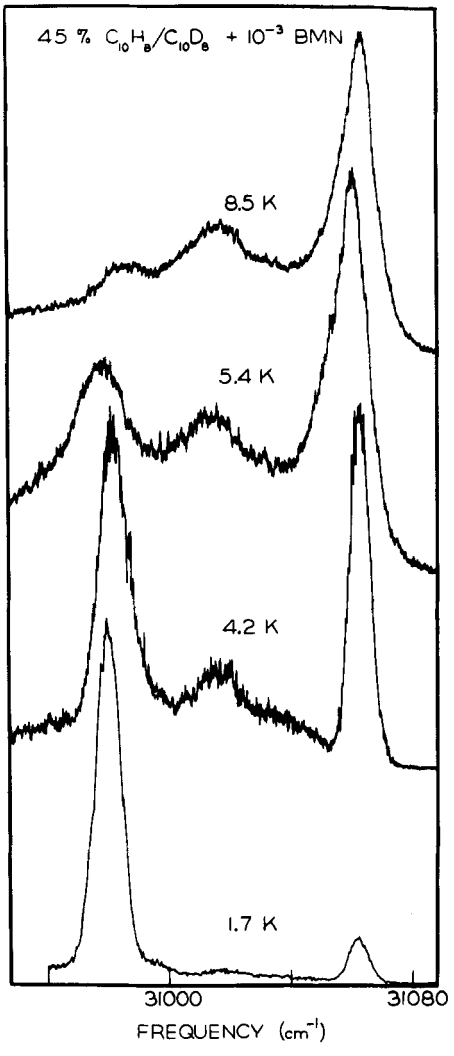

FIGURE 11 Temperature dependent dynamic $^1B_{2u}$ exciton percolation for the 45% guest sample. The $C_{10}H_8$ 0-"510" cm^{-1} vibronic band at $\simeq$30,980 cm^{-1} is compared to the intensity of the BMN 0—0 band at 31,063 cm^{-1}. The 1.7 and 4.2 K spectra were taken while the samples were immersed in liquid He, while the 5.4 and 8.5 K spectra were taken in a Janis variable temperature dewar. Note that the peak at $\simeq$31,020 cm^{-1} in the 8.5 K spectrum is a BMN phonon sideband.

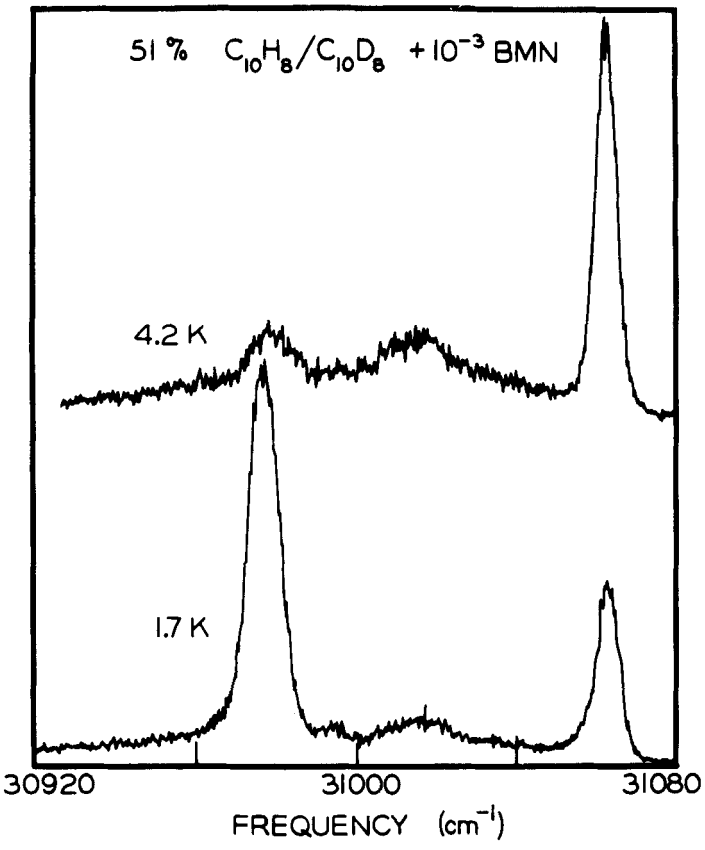

FIGURE 12 Temperature dependent dynamic $^1B_{2u}$ exciton percolation for the 51% $C_{10}H_8$ guest sample. The $C_{10}H_8$ 0-"510" cm^{-1} vibronic band at $\simeq$30,975 cm^{-1} is compared to the intensity of the BMN 0—0 band at 31,064 cm^{-1}. Both the 1.7 and 4.2 K spectra were taken while the samples were immersed in liquid HE. Note that the peak at 31,015 cm^{-1} is a BMN phonon sideband.

From Eqs. 12 and 13 we can estimate that the slope of the curve in Figure 13 at low C_g (below the knee), should equal $(E_h - E_t)/k$ which is just the trap depth in degrees Kelvin. For the $C_{10}H_8/C_{10}D_8$ system (I) we calculate this quantity to be about 70 K. The slope derived from the low C_g points in Figure 13 is $\simeq 77° \pm 20$ K. Thus, it appears justified to say that the dominant mechanism at low C_g is indeed a trap to host-band thermalization.[46] It should be noted that the quantity $(E_h - E_t)$ actually varies[45] from 70 K to 100 K, over the concentration range 1.2%–17%, so there should be some non-linearity in Eq. 12.

The "knee" in Figure 13, located around $C_g = 0.2$, marks the onset of dynamic percolation, *i.e.*, where trap-trap tunneling becomes important.

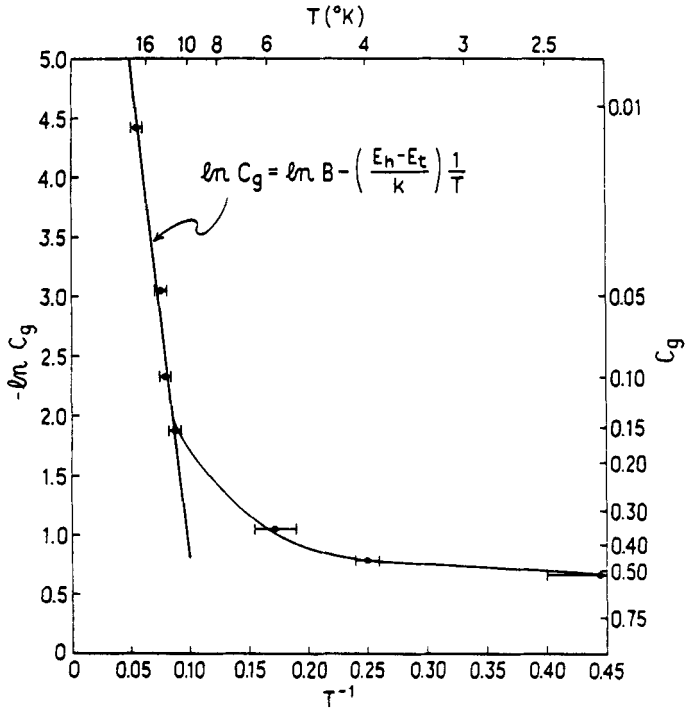

FIGURE 13. Temperature dependence of $^1B_{2u}$ dynamic percolation: $-\ln C_g$ vs. T^{-1}. The inverse of the temperature where $I_{C_{10}H_8} \simeq I_{BMN}$ has been plotted for a range of guest concentrations. The units of temperature are degrees Kelvin and the guest concentration is expressed in terms of mole fraction. The points corresponding to the lower values of the mole fraction guest have been fitted by a straight line (see Eq. 12). The slope, which corresponds to $(E_h - E_t/k)$, is found to be about 77°K, which is the trap depth in degrees Kelvin. Both the value of C_s and $(E_h - E_t)$ are assumed to be independent of the guest concentration. We estimate from the curve that around $C_g \simeq 0.20$, there is a marked departure from linearity signifying the emergence of superexchange tunneling as the dominant transfer mechanism.

In Figure 5 we predicted that, for $C_s \simeq 10^{-3}$, C_g^* (the concentration where the singlet exciton cluster-cluster transfer mechanism becomes important) is $\simeq 20\%$. This is in good agreement with the above experimental value of $\simeq 20(\pm 5)\%$ concentration.

Another manifestation of increasing the temperature can be seen if we examine the detailed spectra for the 35% and 45% guest (e.g. Figures 10, 11) in the region of the "510" vibronic band (approximately 30,980 cm^{-1}). This band is the sum of the emission from a range of cluster sizes.[45] At low temperatures, when $\delta > kT$, the larger, lower energy clusters trap out the majority of the excitons. When the temperature is raised from 4.2 K to 5.6 K in the 35% crystal, or from 1.7 to 4.2 K in the 45% sample, the lower energy edge

of the band, corresponding to emission from the larger clusters, does not appreciably shift; whereas the higher energy edge is blue-shifted at the elevated temperature. The fact that the lower edge remains the same should rule out simple homogenous thermal broadening; rather, the additional kT allows trap-to-trap transfer to previously inaccessible, smaller, higher energy clusters. When $kT \gg \delta$ we expect the line shape to correspond to that of the simple weighted distribution of clusters (compare to Ref. 27). We also expect the population of the higher energy states of the same larger clusters to be increased due to the higher kT, thus the emission from the same would *also* have a blue shifted upper band edge.

Triplet thermalization and percolation

Since the nearest neighbor pairwise interaction energy is much smaller in $^3B_{1u}$ (the first triplet exciton) than $^1B_{2u}$ naphthalene (the first singlet exciton), i.e. 1.25 cm^{-1} compared to 18 cm^{-1}, we would expect the triplet trap-trap migration's *strong* dependence upon the temperature to occur in a lower temperature domain than for the singlet. Indeed, most of the variable temperature experiments analogous to those we performed for the singlet would have to be performed much below 1–2 K, where the Boltzmann factor $\exp[-\delta/kT] \to 1$. Here, again, δ is the difference in energy between the states of two different isolated clusters of interest. The difficulties involved in attaining these low temperatures are sufficient to prompt one to search for alternate methods of studying temperature effects in the triplet state. As mentioned, such a system exists as an 8 cm^{-1} naphthalene-d_8 defect site which is observable at 21,200 cm^{-1} in the phosphorescence spectra of the 8.33% and 9.9% $C_{10}H_8/C_{10}D_8$ samples. The spectra of these samples are shown in Figures 14 and 15. This defect may or may not be present in other samples, depending on the method of preparation, but for reasons to be explained, we expect it to give much weaker emissions in any samples other than those directly above or below the percolation concentration for this system (see however, Ref. 28).

By changing the He bath temperature between 1.7 and 4.2 K, we can change the Boltzmann factor $e^{-\Delta E/kT}$ for an 8 cm^{-1} trap from 1.1×10^{-3} to 6.4×10^{-2}. The consequences of these defect sites at 1.7 and 4.2 K can be analyzed in terms of the effect they have upon the *overall* guest-guest transfer rate. To do this, we estimate, from Table III and $\bar{C}_s$, that the defect concentration is at most $\simeq 1:500$, relative to that of the regular $C_{10}H_8$, and that the overall rate of transfer is proportional to the Boltzmann factor $\exp[-\Delta E/kT]$. At 4.2 K one out of every 500 jumps to a distinct site may be trapped by a defect $C_{10}D_8$ site. The rate of transfer out of these sites is $[6.4 \times 10^{-2}]^{-1}$ times slower, thus the overall rate is slowed by a factor of 1.02. Similarly, at

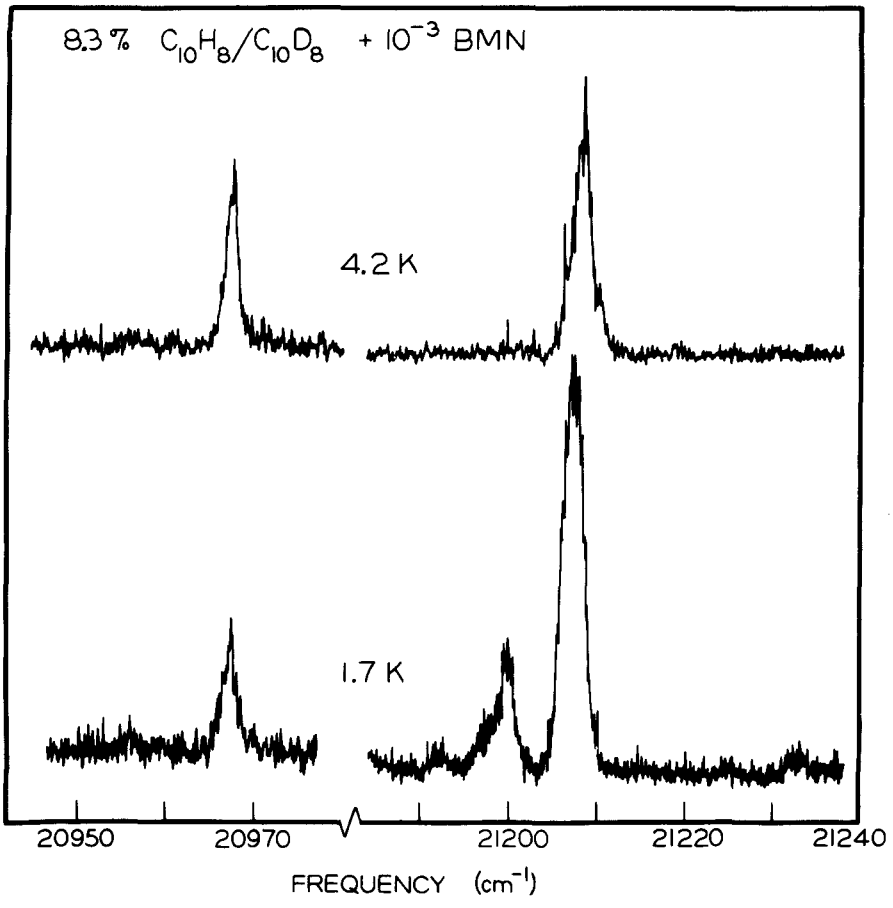

FIGURE 14 Temperature dependence, at 1.7 and 4.2 K, of the intensity of the phosphorescence origins of $C_{10}H_8$ (21,208 cm^{-1}), $C_{10}D_8$-defect (21,200 cm^{-1}) and BMN (20,968 cm^{-1}) for the 8.3% mole fraction $C_{10}H_8$ in $C_{10}D_8$ host plus $\simeq 0.02\%$ BMN sample.

1.7 K these defect sites slow down the rate of transfer (0.2% of the time) by a factor of $[1.1 \times 10^{-3}]^{-1}$, thus the overall rate is slowed down by a factor of 2.8. Therefore, at 4.2 K the defect has very little effect while at 1.7 K the reduced *overall* rate of transfer means that I_s/I_t may be a good deal less than if there were no defects.

For this triplet system, at guest concentrations much below the dynamic percolation concentration, we observe phosphorescence primarily from small clusters of naphthalene, some from BMN and little or no emission from the defect sites. Defect phosphorescence was not observed in samples where $C_g \ll 8.3\%$. At these concentrations the rare, lower-energy defect sites

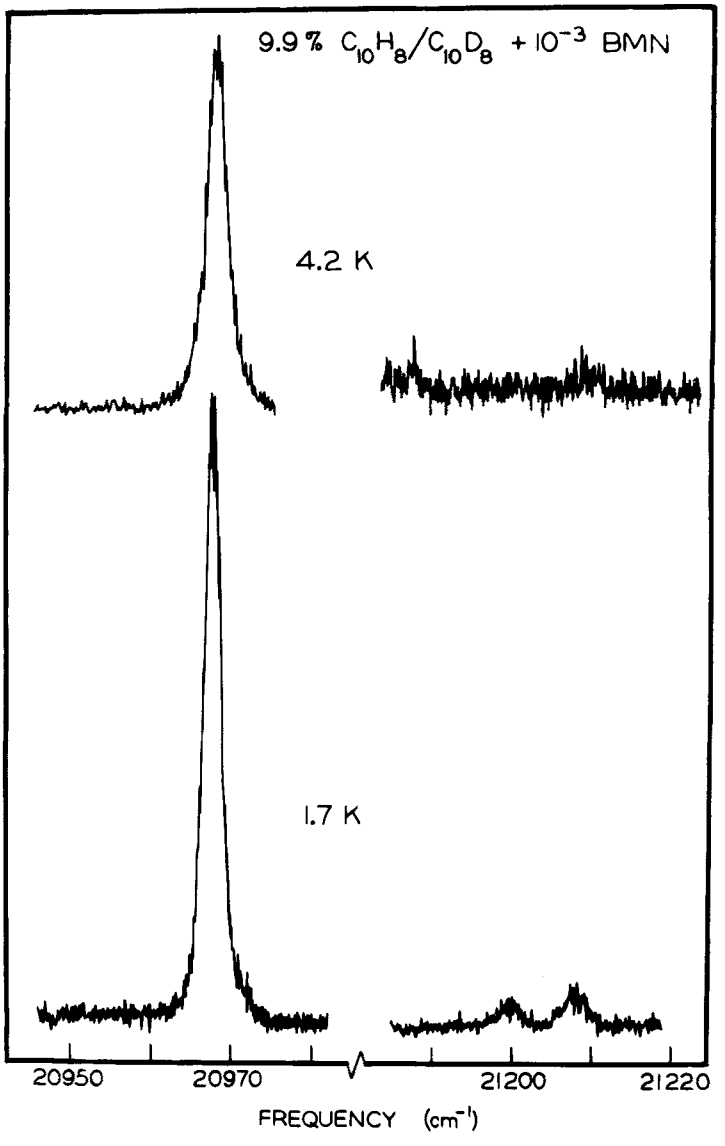

FIGURE 15 Temperature dependence, at 1.7 and 4.2 K, of the intensity of the phosphorescence origins of $C_{10}H_8$ (21,208 cm^{-1}), $C_{10}D_8$-defect (21,200 cm^{-1}) and BMN (20,968 cm^{-1}) for the 9.9% mole fraction $C_{10}H_8$ in $C_{10}D_8$ host plus $\simeq$0.09% BMN sample.

are isolated from other trap molecules and thus compete for the excitons with the more abundant BMN *and* naphthalene clusters. The phosphorescence from any species, well below percolation, is nearly proportional to its relative concentration.[47] The defect emission has been seen in some very recent studies by Ahlgren, with a much lower BMN concentration,[28] but disappeared for samples prepared from potassium fused naphthalene (host and guest). We note, however, that very weak emissions at 8 cm^{-1} below the $C_{10}H_8$ origin were observed by Ochs[33] on samples with potassium fused $C_{10}D_8$ host.

The integrated intensities of the $C_{10}H_8$ origin, $C_{10}D_8$ defect origin and the BMN origin for 8.3% guest are given in Table III. As mentioned earlier, the Boltzmann factor at 1.7 K indicates a small probability of thermal excitation from a defect-localized exciton to the $C_{10}H_8$ "band", for the 8.33% sample. When thermal excitation does occur, the exciton is often retrapped in the defect site since C_g is just below percolation. If the temperature of the crystal is raised to 4.2 K, the defect emission disappears and there is much more BMN emission relative to $C_{10}H_8$ (see Table III). The probability of thermal detrapping from the defect site has increased by about two orders of magnitude. This would, in itself, decrease the emission from defect sites relative to the more abundant $C_{10}H_8$ and BMN species. The increase in temperature also increases the efficiency of trap-trap migration. The splitting in energy between guest clusters of different size reduces the efficiency of trap-trap migration in the triplet as it did in the singlet. However, at 4.2 K, where $kT \cong 2.6\ cm^{-1}$, and $\delta < 1.25\ cm^{-1}$, the individual cluster states can be thought of as being in a guest quasi-band, accessible through the increased number of phonon states at that temperature. This increase in trap-trap migration leads to a greater number of guest sites visited by an exciton and, consequently, to an increase in the relative BMN emission. This is indeed observed. The 9.9% sample at 1.7 K also shows some defect emission (Figure 15) with the intensity ratios shown in Table III. The first thing that we notice is the large relative amount of BMN emission at both temperatures compared to the 8.3% sample. The explanation for this is simply that we have attained dynamic percolation at this concentration. The fact that we still observe some

TABLE III

Integrated relative guest phosphorescent intensities

	8.33%		9.9%	
Guest Species	1.7 K	4.2 K	1.7 K	4.2 K
$C_{10}H_8$ (21,208 cm^{-1})	0.57	0.43	0.07	0.02
$C_{10}D_8$ (defect) (21,200 cm^{-1})	0.17	—	0.04	—
BMN (20,968 cm^{-1})	0.26	0.57	0.89	0.98

residual $C_{10}H_8$ phosphorescence indicates that there are still finite clusters of $C_{10}H_8$ which have not yet percolated and contain no BMN. If this is the case, then one would expect to see *some* defect phosphorescence at this temperature as long as $C_{10}H_8$ phosphorescence is observed. When the temperature of this crystal is raised to 4.2 K, only a very small fraction of the total phosphorescence is from $C_{10}H_8$ (< 2%) and the defect phosphorescence is not observable. The same arguments apply here as did for the 8.3% sample at 4.2 K, except that now, at 9.9%, C_g is above percolation and the frequent detrapping of the defect excitons almost always leads to BMN trapping of the exciton. At concentrations $\gg C_c^s$, even at 1.7 K, we would not expect to see any defect emission. Despite the small Boltzmann factor at 1.7 K, the long triplet lifetime and the existence of large maxi-clusters above percolation do insure that even an infrequently detrapped defect exciton will eventually be trapped out by a supertrap site within its lifetime. In contrast, the Boltzmann factor for BMN detrapping ($\exp[-240/1.18] = 10^{-88}$) ensures that once an exciton at 1.7 K is trapped by BMN, it stays trapped within its lifetime. We note that the defect sites should be treated as supertraps additional to BMN, for the sake of the dynamic percolation problem. Thus, the I_s value for the 8.3 and 9.9% samples should include I_{BMN} and I_{defect}. Further temperature studies on this system are given elsewhere.[28]

We note here that we have also observed in our laboratory[5a,33,48] both thermalization and a combination of thermalization and dynamic percolation in another naphthalene triplet system (Table I, system V) made of $C_{10}D_8$ host, $C_{10}D_4H_4$ "trap" and supertraps of $C_{10}D_3H_5$, $C_{10}D_2H_6$, $C_{10}DH_7$, $C_{10}H_8$ and BMN. Here the guest-host energy separation ($27\ cm^{-1}$)[5a] is smaller than in our systems I–IV, enabling guest-host thermalization at temperatures as low as 2 K. The thermalization mechanism has been borne out by a temperature study[48] up to 24 K. Again, in stages, the higher supertraps lose their energy to the lower ones (presumably by a two-stage thermalization, first to the "trap", then to the "host"). Eventually, at the highest temperature studied, all emission comes from the lowest energy supertrap, BMN. A similar energy cascade and thermalization study has been reported on the biphenyl system.[49]

Thermal erosion of percolation

How low can a critical concentration for energy transport occur? Looking at Eq. 5, and assuming $kT > \beta$, we can increase $\bar{n}$ (and thus decrease C_c) upon increases of $\bar{C}_s$ (but $\bar{C}_s \ll 1$ is a must), or t (i.e. the lifetime τ), or β (determined by the system), or a decrease of Δ (obtainable via isotopic substitution). Eventually, however, the competing, non-percolating, energy transport via guest-host thermalization will put a limit to lowering C_c by eroding the

percolation process. This is especially true for a reduction of Δ, as $\Delta \simeq E_h - E_g$ and the thermalization is proportional to $\exp[-(E_h - E_g)/kT]$. (Such erosion was indeed observed for system V, see above). The same obviously goes for an increase in temperature, which initially reduces C_c due to the decrease in $\exp(-\delta/kT)$, but eventually erodes the critical percolation concentration due to guest-host thermalization as exhibited by our singlet results.

LOCALIZATION VS. DELOCALIZATION

1. Localization and thermalization

We have seen above, and in earlier work[5a] that *triplet* percolation occurs without much complication due to trap ($C_{10}H_8$) localization. At about the critical percolation concentration for System I (8%), much of the $C_{10}H_8$ monomer excitation will be *temporarily* trapped by the lower energy states of the dimers, trimers, etc. This has been explicitly observed by Braun and Wolf[50] in a pure $C_{10}H_8$-$C_{10}D_8$ system (i.e., *no* supertrap). We also know that the concentration of such cluster species is neither negligible, nor large enough to percolate on its own: Out of 8.3% total $C_{10}H_8$ guest one has[5b] 5.9% monomer $C_{10}H_8$, 1.6% dimer, 0.6% trimer, 0.2% tetramer, etc. In view of the fact that the cluster state differential energy, δ, is about 1 cm^{-1} or less for the triplet state excitons in System I *and* that $kT \geq \delta$ at the working temperature of 1.7 K, we conclude that cluster to cluster thermalization is highly probable. Whether the "phonon assist" involves direct phonon annihilation or a Raman type process[51] is beyond the scope of our present discussion.

A very similar thermalization process is also exhibited by the "defect" naphthalene species (in the 8.3 and 9.9% guest samples), which is 8 cm^{-1} below the monomer level. Whenever kT is sufficient, these trap excitons are also thermalized back into the "impurity" band. Finally, the "orientation splitting" in the 1-$DC_{10}H_7$ samples[35] (~ 1 cm^{-1}) in System IV had no apparent effect on the percolation concentration. Thermalization appears to be fast enough in *all* these cases, and thus is definitely not the "bottle-neck" in the energy transfer process.

2. Localization energy vs. impurity bandwidth

The triplet dimer state is 1.25 cm^{-1} *below* the "monomer band," which has an expected bandwidth B of only about[52] 10^{-6} cm^{-1} at percolation (see below). These dimers are also statistically distributed, i.e., they should be present *at random* in each one of the sample's domains. As stated above, this

very large ratio of δ/B does not prevent thermalization. The above estimate for B assumes no Anderson localization.[3]

3. Anderson localization and thermalization

Any localization energy due to host lattice inhomogeneities ("Anderson" localization)[8–12] should be well below 1 cm^{-1}. This is based on the following: (a) The observed spectral linewidths are sharper than 1 cm^{-1}. (b) We expect the small domain in which energy transfer is operating (about[5,52] 10^3 Å) to be much more homogeneous than the bulk crystal. Thus, at $T \geq 1.5$ K, we expect thermalization to overcome any "Anderson localization" i.e., any "break-up" of the exciton band into "localized levels". This topic has been much discussed elsewhere.[52–55]

4. Inhomogeneous broadening and intradomain energy transfer

We like to emphasize that even without thermalization (or at 0°K) energy transfer inside a domain is possible, according to the Anderson criteria,[12] as long as the *intradomain energy inhomogeneity* is not significantly larger than the exciton impurity bandwidth B. It is reasonable to assume that most of the bulk crystal "inhomogeneous linebroadening" could be due to *inter*-domain imperfections, rather than to *intra*-domain inhomogeneities. This has also been recently discussed by Colson.[56]

5. Singlet exciton cluster localization

As pointed out earlier, the cluster (dimer, trimer, etc.) localization energy for the singlet case is of the order of 15–30 cm^{-1}. At the lowest temperature experiments (1.5°K), this localization energy δ is large compared to kT. Obviously, here we rely on defining the "clusters" by the nearest neighbor (square lattice) topology.[5,18] It is reasonable to believe that for $\delta \simeq kT$, i.e. at our higher temperatures,[57] thermalization again occurs. We note that for $\delta = 18\ cm^{-1}$ and $T = 1.7$ K the Boltzmann factor is 10^{-6}, thus giving a "dimer" to "monomer" jump-time[58] of about several lifetimes (*vide infra*).

6. The analog-Anderson–Mott localization

We can see that singlet exciton cluster localization will break up the singlet exciton "impurity band" and thus limit the energy transfer. This is analogous to the Anderson–Mott localization. However, the difference lies in the fact that the source of the localization energy is *not* an external (host) perturbation. Rather it is an *internal* "perturbation", having to do with the (off-diagonal)

exciton interactions. These perturbations are easy to predict, as they are based on the values of the exciton-exchange interactions.[17] This problem has already been discussed in detail before.[5b] However, we want to emphasize the difference between this kind of localization and the traditional "Anderson" localization, which we have long ago recognized as a potential "spoiler" for exciton percolation.[24]

We were able to account *semiquantitatively* for the difference in percolation concentration C_c between our low temperature (1.5°K) experiments and the elevated temperature experiments (where kT is "large enough"). This had to do with the difference between the nominal guest concentration C_g and the effective guest concentration C_g'. If, at *low temperatures*, we exclude from our "energy conducting species" ($C_{10}H_8$) the small clusters whose lowest energies are δ (15–30 cm^{-1}) above the bottom of the "impurity band", i.e., excluding monomers, dimers, trimers, tetramers and some larger clusters, the concentration C_g' of the exciton conducting species is reduced from, say, 45% to about 30%. (For a fuller discussion see Ref. 5b).

Off-diagonal inhomogeneities and their "negative" effects on localization have been discussed by Antoniou and Economou[59,60] and recently by Klafter and Jortner.[3] These differ from our case, where the off-diagonal inhomogeneities are determined by the cluster structure of the crystal. The cluster structure, in turn, is completely defined by the static percolation theory. Thus, to speak of "analog off-diagonal Anderson localization" is equivalent to speaking of static percolation[52] or rather de-percolation. Practically, speaking about a system like naphthalene, it is obvious that the very large clusters (defined by the nearest neighbor square lattice topology), suddenly fall apart, just about the limiting percolation concentration of 0.593. This creates a sudden sharp increase in off-diagonal inhomogeneities, which is somewhat analogous to an Anderson localization. The falling apart of the large clusters and the concomitant increase in off-diagonal inhomogeneities affects, first of all, the static properties like the absorption spectrum and the exciton density of states.[2] It also affects the "dynamic exciton percolation", i.e., energy transfer, whenever the thermalization *cannot* overcome this off-diagonal inhomogeneity. This model of "analog Anderson localization" has been discussed by us in terms of the "off-diagonal inhomogeneity" δ, the band parameters β and the thermal energy kT, for both the triplet and singlet naphthalene case,[52] and in greater detail for the singlet case,[5b] where $kT \ll \delta$ at our lowest experimental temperatures. The same problem has also been discussed for benzene, by Colson *et al.*,[6,56] and may have been implied for some other systems by Zewail *et al.*[7,61] In the latter case it should have been realized that only below the critical percolation concentration can such *analog* Anderson localization happen. Obviously, for one-dimensional exciton interaction topologies any mixed crystal is below the critical percola-

tion concentration (of unity). On the other hand it is expected that real crystals will seldom exhibit truly one-dimensional exciton transfer. However, the primary cluster topology, or major "off-diagonal inhomogeneity", may well exhibit such a behavior, like in the case of the first triplet exciton of dibromonaphthalene.[7,61]

Finally, to avoid confusion, we like to emphasize the crucial distinction between the *original* Anderson localization model, related to the local inhomogeneity W of the diagonal site excitation energy,[3,12] and our "analog" localization model,[5b] related to a special kind of "off-diagonal" inhomogeneity, i.e., to the distribution in primary cluster energies. In the first case one has *two* independent parameters, which are juxtaposed: The local inhomogeneity or energy "spread" W and the bandwidth parameter B, which in our case of short range interactions can be replaced by the *primary* exciton transfer integral β for the pure crystal (or J_n for the mixed one). It is the order of magnitude of the *ratio* W/β or W/J_n which is all important. However, in the "analog" localization case, the "inhomogeneous energy-spread δ" is given by the "off-diagonal inhomogeneity", which is given, in turn, by the *primary* exciton transfer integral β itself! Thus, δ/β is usually of the order of unity! Furthermore, one *always has* $\delta < B$ above the primary percolation concentration (0.593). Thus, the situation is qualitatively different and quantitatively very subtle. There is apparently *one* independent parameter. For the case of only direct exciton exchange we have discussed the subtle juxtaposition of δ with the secondary (i.e., next nearest neighbor) exciton transfer integral β'. For indirect exciton exchange (tunneling) one actually compares $\delta \approx \beta$ with $\beta(\beta/\Delta)^{n-1}$, where Δ is a "trapdepth" (isotopic guest-host energy separation) and n is the smallest number of primary bonds connecting the two "traps", or δ/β with $(\beta/\Delta)^{n-1}$. One could claim that one just "inverted" the role of inhomogeneities and band-parameters by considering now the guest-host separation as the "effective inhomogeneity". This is not only artificial, but neglects the all important role of the exponent $(n-1)$. Moreover, it is this parameter n which defines our *long range percolation*, i.e., the purely mathematical critical percolation concentration, as given implicitly in Figure 1. These critical percolation concentrations C_c^n have been evaluated by us[5a,16] and by Colson *et al.*[7] Actually, more rigorously (see Eq. 3), δ/β should be compared with

$$\bar{\Gamma}_n\left(\frac{\beta}{\Delta}\right)^{n-1} \tag{14}$$

where $\bar{\Gamma}_n$ is again a function of n. It thus becomes obvious that the *analog Anderson localization*, using the so-called off-diagonal inhomogeneity, does *not* possess a clear-cut independent parameter δ describing the local inhomogeneity. For *direct* exciton transfer this δ is *determined* by the *exciton band*

dispersion relation. Furthermore, $\delta \to 0$ well above the primary critical percolation concentration.

In addition, for our case of "deep trap" guest excitons, the "analog Anderson criterion" is destined to result in localization below the primary percolation concentration (for $T \to 0$), as the ratio given in Eq. 14 is *always* small compared to unity, resulting in quasi-static percolation for $\delta > kT$. The opposite regime is given by $\delta < kT$, i.e., where thermalization prevents permanent exciton localization, thus bringing us back to our physically interesting limit of dynamic exciton percolation, where *time* (e.g., the exciton lifetime) plays a major role (see below).

7. Percolation theory and 'impurity bandwidths'

Any theoretical estimate of the "impurity" bandwidth, at given impurity concentration, depends on a correct *average* distance between impurities. For instance, for the triplet exciton critical percolation concentration of 0.08 mole fraction we have an "average maximum" inter-impurity spacing (n) of 4 to 5 (see above and Figure 4). This gives a pairwise tunneling interaction ($J_n = \overline{\Gamma}_n \beta^n / \Delta^{n-1}$) or bandwidth B of about $10^{-6}\,\mathrm{cm}^{-1}$. Using the very same parameters (δ and β), Klafter and Jortner[3] got a result higher by many orders of magnitude, mainly because they derived a value of n that seems to us[52] to be based on an unsatisfactory statistical procedure. Specifically, their "average" distance is heavily weighted (in the downward direction) by nearest neighbor distances found inside dimers, trimers, and other small clusters, which are irrelevant to the definition of an infinitely extended state. Such dimers and trimers do contribute to an energy "spread" but not to a true "bandwidth" in the sense of the usual definition of a band in solid state theory.[8–12]

8. The time factor

In the simple Anderson localization model[3,12] time is *not* a factor. There either is a band, giving transfer, or there is no band. However, at temperatures above 0 K one can get an effective Anderson transition which will just "slow down" the transfer. Even more important is the effective *analog* Anderson transition. It is the latter which we believe becomes important *if* the following conditions are met: (a) The concentration is below the critical percolation concentration, as defined by the *primary* exciton interaction topology (i.e., square lattice for naphthalene). (b) The primary band parameter β (primary exciton interaction) is large compared to kT. If both of these conditions are met then the exciton transfer time is significantly determined by phonon assisted thermalization—a still largely virgin field of

investigation.[7,51] However, when condition (b) is not met, then the energy transfer time should be described quantitatively by our formalism (Eqs. 5 and 6) of exciton percolation via tunneling (superexchange) with only minor temperature effects.[28] Thus, quantitative time-resolved exciton transfer studies are the key for a further refinement of our theoretical models, i.e., the choice between a dynamic percolation via tunneling model and a static Anderson-localization via diagonal inhomogeneous broadening. Such studies are now underway.[55]

Finally, we note that when condition (a) is not met, i.e., above the "primary" critical percolation concentration (i.e., above 0.593 mole fraction for naphthalene), direct exciton exchange effectively replaces tunneling. Here one expects little time dependence in the exciton "supertransfer" limit,[5a,21] i.e., medium-range energy transport, but time is again at a premium for long range energy transport due to the finite rate of the direct exciton transfer.[37,62]

CONCLUSIONS

A wealth of data is shown to be in reasonable quantitative agreement with the *exciton tunneling percolation model* for all cases where *both the "diagonal" and the "off-diagonal"* energy *"inhomogeneity"* δ is *small relative to the thermal energy* kT. Not using freely adjustable parameters we get at least an order of magnitude agreement with dozens of independent experimental parameters. The timescale of the energy transfer experiment is shown to be the primary factor in exciton percolation. This enables a coexistence between quantum mechanical tunneling and the "classical" percolation approach, which defines the (time dependent) lattice connectivity. In our naphthalene systems we find no evidence for Anderson localization due to diagonal inhomogeneities. However, the *analog Anderson localization*, due to off-diagonal "inhomogeneities" (cluster effects), takes over at very low temperatures, thus assuring that, at the limit of $T \to 0$, the dynamic percolation concentration approaches the static percolation concentration, which in turn is defined by the primary cluster topology. This primary topology is the square lattice, in our case of naphthalene, as it is based only on the nearest neighbor, interchange equivalent, exciton exchange interactions.

We believe that *effective exciton localization* (absence of energy transport) in these systems occurs when $kT \ll \beta$ (β being the pairwise excitation exchange term) rather than at the Anderson–Mott transition, $B < W$, where B is an effective bandwidth and W is a local disorder. One reason for the above is that for these systems we have the relation $\beta \gg W$. If the latter relation were reversed, our "effective exciton localisation" (absence of energy transport)

would probably occur when $kT \ll W$, with little guest concentration dependence. Our more quantitative description incorporates as a primary factor the term $\beta\tau$, where τ is the monomolecular decay time. The fact that $\beta\tau$ is about 10^6 times larger for the triplet than the singlet excitation is responsible for the occurence of triplet dynamic percolation at much lower guest concentrations. The above assumes that "all else" is about equal, including the ratio β/kT, and implies no significant guest-host thermalization.

It is not clear to us whether our energy transport systems will show an Anderson–Mott transition at a "low enough" temperature, which is then "eroded" by a temperature increase, as suggested by Klafter and Jortner.[30] We believe, however, that we did indeed observe here a thermal erosion of the quasistatic percolation for the singlet system, resulting in a dynamic percolation at lower concentration. We also definitely observed the expected thermal erosion of the dynamic percolation, due to guest-host thermalization, for both singlet and triplet systems.

References

1. V. L. Broude and E. I. Rashba, *Pure and Appl. Chem.*, **37**, 21 (1974) and references therein.
2. H-K. Hong and R. Kopelman, *J. Chem. Phys.*, **55**, 3613 (1971).
3. (a) J. Klafter and J. Jortner, *Chem. Phys. Lett.*, **49**, 410 (1977). (b) J. Klafter, *Ph.D. Thesis*, Tel-Aviv University (1978). (c) J. Klafter and J. Jortner, *Chem. Phys. Lett.*, **60**, 5 (1978).
4. A. Blumen and R. Silbey, *J. Chem. Phys.*, **70**, 3707 (1979).
5. (a) R. Kopelman, E. M. Monberg, and F. W. Ochs, *Chem. Phys.*, **19**, 413 (1977). (b) R. Kopelman, E. M. Monberg, and F. W. Ochs, *Chem. Phys.*, **21**, 373 (1977).
6. (a) S. D. Colson, R. E. Turner, and V. Vaida, *J. Chem. Phys.*, **66**, 2187 (1977). (b) S. D. Colson, S. M. George, T. Keyes, and V. Vaida, *J. Chem. Phys.*, **67**, 4941 (1977).
7. (a) D. D. Smith, R. D. Mead, and A. H. Zewail, *Chem. Phys. Lett.*, **50**, 358 (1977). (b) D. M. Burland and A. H. Zewail, *Adv. Chem. Phys.*, (in press).
8. P. W. Anderson, Nobel Address, *Rev. Mod. Phys.*, **50**, 191 (1978).
9. N. F. Mott, *ibid.*, **50**, 203 (1978).
10. S. K. Lyo, *Phys. Rev. B*, **3**, 3331 (1971).
11. R. Orbach, *Phys. Lett.*, **A48**, 417 (1974).
12. P. W. Anderson, *Phys. Rev.*, **109**, 1492 (1958).
13. S. Chandrasekhar, *Rev. Mod. Phys.*, **15**, 1 (1943).
14. (a) S. W. Haan and R. Zwanzig, *J. Chem. Phys.*, **68**, 1879 (1978). (b) D. J. Thouless in Les Houches, Session XXXI, 1978—Condensed Matter, R. Balian *et al.*., eds., North–Holland (1979).
15. V. K. S. Shante and S. Kirkpatrick, *Adv. Phys.*, **20**, 325 (1971).
16. J. Hoshen, R. Kopelman, and E. M. Monberg, *J. Stat. Phys.*, **19**, 219 (1978).
17. R. Kopelman, Excited States Vol. 2, ed. E. C. Lim (Academic Press, New York, 1975) p. 33.
18. R. Kopelman, Radiationless Processes in Molecules and Condensed Phases, Topics in Applied Physics Vol. 15, ed. F. K. Fong (Springer, Berlin, 1976) p. 297.
19. Y. Shinozuka and Y. Toyozawa, preprint (1978).
20. R. Kopelman, E. M. Monberg, F. W. Ochs, and P. N. Prasad, *Phys. Rev. Lett.*, **34**, 1506 (1975).
21. R. Kopelman, E. M. Monberg, F. W. Ochs, and P. N. Prasad, *J. Chem. Phys.*, **62**, 292 (1975).
22. H-K. Hong and R. Kopelman, *J. Chem. Phys.*, **55**, 724 (1971).
23. E. M. Monberg, Ph.D. Thesis, Univ. of Michigan, Ann Arbor (1977).
24. J. Hoshen and R. Kopelman, *J. Chem. Phys.*, **65**, 2817 (1976).

25. R. Kopelman, *J. Phys. Chem.*, **80**, 2191 (1976).
26. J. Hoshen and R. Kopelman, *Phys. Rev.*, **B14**, 3438 (1976).
27. J. Hoshen and R. Kopelman, *Phys. Stat. Sol.*, **B81**, 479 (1977).
28. D. C. Ahlgren, Ph.D. Thesis, Univ. of Michigan, Ann Arbor (1979).
29. D. M. Hanson, *J. Chem. Phys.*, **51**, 5063 (1969).
30. (a) B. J. Botter, C. J. Nonhoff, J. Schmidt, and J. H. Van der Waals, *Chem. Phys. Lett.*, **43**, 210 (1976). (b) F. Dupuy, Ph. Pee, R. Lalanne, J. P. Lemaistre, C. Vaucamps, H. Port, and Ph. Kottis, *Mol. Phys.*, **35**, 595 (1978).
31. R. Kopelman and J. C. Laufer, Electronic Density of States, ed. L. H. Bennett, National Bureau of Standards Special Publication No. 323 (U.S.G.P.O., Washington, D.C., 1971) p. 261.
32. L. Altwegg, M. Chabr, and I. Zschokke-Gränacher, *Phys. Rev.*, **B14**, 1963 (1976).
33. F. W. Ochs, Ph.D. Thesis, Univ. of Michigan, Ann Arbor, (1974).
34. E. R. Bernstein, S. D. Colson, R. Kopelman, and G. W. Robinson, *J. Chem. Phys.*, **48**, 5596 (1968).
35. F. W. Ochs, P. N. Prasad, and R. Kopelman, *Chem. Phys.*, **6**, 253 (1974).
36. There has been a long-standing question on whether to use for a "jump-time" or a "transfer time" an expression like Eq. 4 or one where J_n is modified by another factor of the form J_n/Γ, where Γ is a measure of the fluctuations due to phonons or is related to the homogeneous linewidth in this system (about 0.01 cm^{-1}, H. Port, private communication, 1978). The choice between J and J^2/Γ type expressions depends not only on whether the transfer is "coherent" or "incoherent," but also on whether the J itself is "bare" or "clothed" and what one means by the above terms. We note that our J values are *experimental* ones (derived from Davydov and cluster splittings) and are thus "clothed" in our terminology. Also, for transfer based on superexchange interactions it is customary[6] to use the linear term, as originally proposed by Nieman and Robinson [G. C. Nieman and G. W. Robinson, *J. Chem. Phys.*, **37**, 2150 (1962)]. This problem is discussed in more detail elsewhere,[28] but even the data listed here seem to be inconsistent with a J^2 dependence, as a comparison of n(exper.) of systems II and IV (Table II) reveals (assuming an identical Γ).
37. P. Argyrakis and R. Kopelman, *J. Theo. Bio.*, **73**, 205 (1978).
38. P. Argyrakis, Ph.D. Thesis, Univ. of Michigan, Ann Arbor (1978).
39. C. Domb and M. Sykes, *Phys. Rev.*, **122**, 77 (1961).
40. C. Domb and N. W. Dalton, *Proc. Phys. Soc.*, **89**, 859, 873 (1966).
41. F. W. Ochs and R. Kopelman, *J. Chem. Phys.*, **66**, 1599 (1977).
42. D. M. Hanson, R. Kopelman and G. W. Robinson, *J. Chem. Phys.*, **51**, 212 (1969).
43. This is a rough value. The actual value is about[28] 128 ns. See also Ref. 55.
44. R. LeSar and R. Kopelman, *Chem. Phys.*, **29**, 289 (1978).
45. (a) P. Argyrakis, E. M. Monberg, and R. Kopelman, *Chem. Phys. Lett.*, **36**, 349 (1975). (b) H. Port, D. Vogel, and H. C. Wolf, *Chem. Phys. Lett.*, **34**, 23 (1975).
46. It is obvious that this system, for the temperatures which we studied, does not reach the equilibrium position of Eq. 7 where the predicted slope $\Delta'/k \simeq 800$. We estimate that the intercept B of the straight line segment in Figure 13 is 9 ± 2. Thus we can write

$$\ln B \simeq 9 \simeq \ln\left[\frac{\alpha C_s \tau_t F'}{t_j}\right].$$

We know[23] that αC_s is about 2×10^{-3} for our system and τ_t/t_j is 2×10^5, approximately,[37] thus giving a value for the modified Franck–Condon factor F' of about 10^{-6}. However, the extrapolation leading to the values of B and F' is quite dubious.
47. Corrections are necessary due to different trapping efficiencies, quantum efficiencies and spectral windows.[23,28]
48. P. N. Prasad, F. W. Ochs, and R. Kopelman, unpublished.
49. P. S. Friedman, P. N. Prasad, and R. Kopelman, *Chem. Phys.*, **13**, 121 (1976).
50. C. L. Braun and H. C. Wolf, *Chem. Phys. Lett.*, **9**, 260 (1971).
51. (a) T. Holstein, S. K. Lyo, and R. Orbach, *Phys. Rev.*, **B15**, 4693 (1977). (b) T. Holstein, S. K. Lyo, and R. Orbach, preprint (1978).

52. E. M. Monberg and R. Kopelman, *Chem. Phys. Lett.*, **58**, 497 (1978).
53. R. Kopelman, E. M. Monberg, J. S. Newhouse, and F. W. Ochs, *J. Luminesc.*, **18/19**, 41 (1979).
54. D. C. Ahlgren and R. Kopelman, *J. Chem. Phys.*, **70**, 3133 (1979).
55. D. C. Ahlgren, E. M. Monberg, and R. Kopelman, *Chem. Phys. Lett.*, **64**, 122 (1979).
56. S. D. Colson and R. Kopelman, unpublished. See also Ref. 6.
57. Such temperatures as defined for each concentration above 20% in Figure 13.
58. Using a "detailed balance approach" (see also Ref. 14b and 51) and a jump time[38] of about 10^{-12} s.
59. E. N. Economou and P. D. Antoniou, *Solid State Commun.*, **21**, 285 (1977).
60. P. D. Antoniou and E. N. Economou, *Phys. Rev.*, **B16**, 3768 (1977).
61. A. H. Zewail, preprint (1979). See also Ref. 7b.
62. P. Argyrakis and R. Kopelman, *Chem. Phys. Lett.*, **61**, 187 (1979).
63. P. Hartman, Phys. and Chem. of Organic Solid State, ed. D. Fox, M. M. Labes and A. Weissberger, (Wiley-Interscience, New York, 1963) p. 390.
64. H. Port, D. Vogel, and H. C. Wolf, *Chem. Phys. Lett.*, **34**, 23 (1975).